

Spring 2020

Effects of Phytoplankton Composition and Biominerals on the Episodic Pulses of Particulate Organic Carbon to Abyssal Depths

Cynthia Michaud
California State University, Monterey Bay

Follow this and additional works at: https://digitalcommons.csumb.edu/caps_thes_all

Recommended Citation

Michaud, Cynthia, "Effects of Phytoplankton Composition and Biominerals on the Episodic Pulses of Particulate Organic Carbon to Abyssal Depths" (2020). *Capstone Projects and Master's Theses*. 841. https://digitalcommons.csumb.edu/caps_thes_all/841

This Master's Thesis (Open Access) is brought to you for free and open access by the Capstone Projects and Master's Theses at Digital Commons @ CSUMB. It has been accepted for inclusion in Capstone Projects and Master's Theses by an authorized administrator of Digital Commons @ CSUMB. For more information, please contact digitalcommons@csumb.edu.

EFFECTS OF PHYTOPLANKTON COMPOSITION AND BIOMINERALS
ON THE EPISODIC PULSES OF PARTICULATE ORGANIC CARBON TO
ABYSSAL DEPTHS

A Thesis
Presented to the
Faculty of
Moss Landing Marine Laboratories
California State University Monterey Bay

In Partial Fulfillment
of the Requirements for the Degree
Master of Science
in
Marine Science

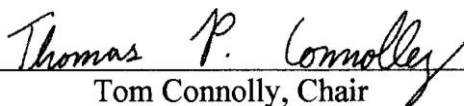
by
Cynthia Michaud
Spring 2020

CALIFORNIA STATE UNIVERSITY MONTEREY BAY

The Undersigned Faculty Committee Approves the

Thesis of Cynthia Michaud:

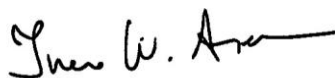
EFFECTS OF PHYTOPLANKTON COMPOSITION AND BIOMINERALS ON
THE EPISODIC PULSES OF PARTICULATE ORGANIC CARBON TO
ABYSSAL DEPTHS



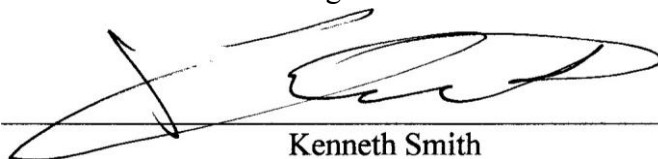
Tom Connolly, Chair
Moss Landing Marine Laboratories



Colleen Durkin
Moss Landing Marine Laboratories



Ivano Aiello
Moss Landing Marine Laboratories



Kenneth Smith
Monterey Bay Aquarium Research Institute



Kris Roney, Dean
Associate VP for Academic Programs and Dean of Undergraduate and Graduate Studies

11 May 2020

Approval Date

Copyright © 2020

by

Cynthia Michaud

All Rights Reserved

ABSTRACT

Effects of phytoplankton composition and biominerals on the episodic pulses of particulate organic carbon to abyssal depths

by

Cynthia Michaud

Master of Science in Marine Science

California State University Monterey Bay, 2020

Carbon is transported to the deep ocean through physical mixing and gravitational sinking of organic particles. Carbon that sinks to the seafloor is consumed by benthic organisms who rely on the detrital particles as their source of food. Station M is a long-term deep-sea study site in the Northeast Pacific where large episodic pulses of particulate organic carbon (POC) sinking to the sea floor at a depth of 4000 meters have been recorded for the past 30 years. The episodic pulses of POC have increased in frequency and magnitude over the past decade, driving a long-term increase in carbon export observed in sediment traps deployed at this location. The goal of this study is to investigate changes in phytoplankton communities within the sinking particles to provide an indication of the ecological mechanisms associated with the high-flux events and why they might be increasing over time. Samples collected by sediment traps were analyzed by microscopy to determine phytoplankton community composition. Phytoplankton community compositions observed in high-flux samples were significantly different from those in low-flux samples. Particles sinking during low-flux periods were relatively more enriched in phytoplankton cells (higher cell:POC fluxes) compared to particles sinking during high-flux events. When separating intact and fragmented diatom cells only the fragmented diatoms had significantly different community compositions in the high- and low-flux events. Since fragmentation of diatoms was significantly different it suggests that grazing and repackaging of the cells was occurring in the water column as the particles sank. Biogenic silica (BSi) and particulate inorganic carbon (PIC) were measured in the particles to test whether mineral ballasting may be driving the large pulses of POC sinking to depth. BSi:POC was constant with increasing POC flux, while the PIC:POC decreased with increasing POC. This indicates that ecological processes leading to high-flux events involve silicifying phytoplankton more than calcifying phytoplankton at Station M. While the biomineral data does not support the ballast hypothesis, it suggests instead that high POC flux is due to production by diatoms in the surface ocean followed by transformation and repackaging through the mesopelagic food web.

TABLE OF CONTENTS

	PAGE
ABSTRACT	vi
LIST OF TABLES	viii
LIST OF FIGURES	ix
ACKNOWLEDGEMENTS	x
1 INTRODUCTION	1
2 METHODS	9
Samples Collected.....	9
Microscopy	10
Cell Classification.....	11
Cell Flux from Phytoplankton Cells	12
Biogenic Silica	13
Statistical Analysis.....	14
3 RESULTS	17
4 DISCUSSION	30
Conclusions.....	40
REFERENCES	42
A SUPPLEMENTARY INFORMATION	47

LIST OF TABLES

	PAGE
Table 1. The functional groups increasing or decreasing during or after the onset of the event	21
Table 2. SIMPER analysis results of intact cell types that determine dissimilarity	25
Table 3. SIMPER analysis results of fragmented diatom cell types that determine dissimilarity.....	26

LIST OF FIGURES

	PAGE
Figure 1. The biological pump in the ocean. Phytoplankton take up inorganic carbon from the surface of the ocean and fix it into organic carbon. The phytoplankton sink to the deep ocean by physical mixing, aggregate formation, or through fecal pellets. These sinking particles bring the organic carbon down to depth where benthic organisms can use this carbon as a source of food.	1
Figure 2. Left) the location of Station M off the southern coast of California. Right) the POC flux over time. The dashed line represents 1.5 standard deviations above the mean POC flux observed at Station M. The red line indicates the high flux events that have been recorded. The POC flux has increased with time (Credit: Christine Huffard, MBARI).	3
Figure 3. Example micrographs of cells. Top diatom <i>Rhizosolenia</i> , bottom left coccolithophore <i>Emiliana-like</i> , bottom middle coccolithophore <i>Coccolithus-like</i> , bottom right diatom <i>Fragilariopsis doliolus</i>	10
Figure 4. Time series incubation of two sediment trap samples in NaOH to determine the amount of time required to dissolve biogenic silica without lithogenic silica contamination. The red line represents the 1-hour period which was chosen for the method.	14
Figure 5. (A) The total carbon flux over the entire time series (blue line). The red dots indicate the high-flux event samples and the orange dots indicate the low-flux samples. (B) The total cell flux in cell/m ² /day over the time series. (C) The total POC flux normalized to mass flux over the entire time series.	17
Figure 6. The identity of the different types of cells in each sample over the time series. The colors in the legend show the different types of cells and their flux in cells/m ² /day in each sample examined. Asterisk represents high-flux events.	18
Figure 7. A) The relative number flux of intact diatoms; significantly fewer intact diatoms were seen in the high-flux events (p-value <0.001), B) the relative number flux of coccolithophores; significantly fewer coccolithophores were seen in the high-flux events (p-value <0.001), C) Nanoflagellate relative number flux; significantly fewer nanoflagellates were seen in the high-flux events (p-value <0.01).	19
Figure 8. A) Relative carbon flux of intact diatoms; significantly less carbon was transported by intact diatoms during high-flux events B) relative carbon flux of coccolithophores; significantly less carbon was transported by coccolithophores during high-flux events, C) relative carbon flux of nanoflagellates; significantly less carbon was transported by nanoflagellates during the high-flux events.	20

Figure 9. A) The relative number flux of fragmented diatoms; there was no significant difference between fragmented diatom number flux between high-flux events and low-flux periods. B) Fragmented diatom relative carbon flux; there was no significant difference between high-flux events and low-flux periods.....	22
Figure 10. A) Relative carbon flux for live diatom cells separated by size (large and small). B) Relative carbon flux for fragmented diatom cells separated by size (large and small).	23
Figure 11. MDS plot of high flux (red) and low flux (blue) samples. Two significantly different clusters are plotted (p-value = 0.001).....	24
Figure 12. Top left: MDS plot of high-flux intact diatom and low-flux intact diatoms. No significant difference between the 2 groups (p-value = 0.021). Top right: MDS plot of high-flux fragmented diatoms, and low-flux fragmented diatoms. There are 2 distinct groups (p-value = 0.001). Bottom left: MDS plot of high-flux fragmented diatoms and high-flux intact diatoms. No significant difference between the 2 groups (p-value = 0.137). Bottom right: MDS plot of low-flux fragmented diatoms and low-flux intact diatoms. No significant difference between the 2 groups (p-value = 0.216).	27
Figure 13. Regression analysis of Opal (top left) and CaCO ₃ (top right) to test if there was a correlation between high flux events and biominerals. Bottom left shows the ratio of Opal:POC versus POC and bottom right shows the ratio of CaCO ₃ :POC versus POC.	29

ACKNOWLEDGEMENTS

I would like to thank my advisor Colleen Durkin for all her encouragement and support in helping design and carry out this study. Along with my other committee members Tom Connolly, Kenneth Smith, and Ivano Aiello for helping me through the experimentation and writing process and providing critical feedback through each step. Thank you to Kenneth Smith for allowing me to use sediment samples from Station M. Thank you to Christine Huffard for helping me locate and collect the samples needed for my analysis. Thank you to the David and Lucile Packard Foundation and the National Science Foundation for funding the Station M time series. Thank you to the ship and crew members of the Western Flyer. Support for this project was provided by California Sea Grant #R/HCME-37. Finally, I would like to thank my parents and Benjamin for their love and support as I worked towards completion of this publication.

INTRODUCTION

In the ocean, inorganic carbon (CO_2 , HCO_3^- , and H_2CO_3) is transformed to organic carbon through photosynthesis and exported to depth by sinking particles in a process called the biological pump (Volk and Hoffert, 1985). Many mechanisms are involved in the eventual transport of carbon to depth, including physical mixing, ecological interactions, and gravitational settling (Ducklow et al., 2001). Phytoplankton take up inorganic carbon from the surface of the ocean and can form aggregates or be ingested by

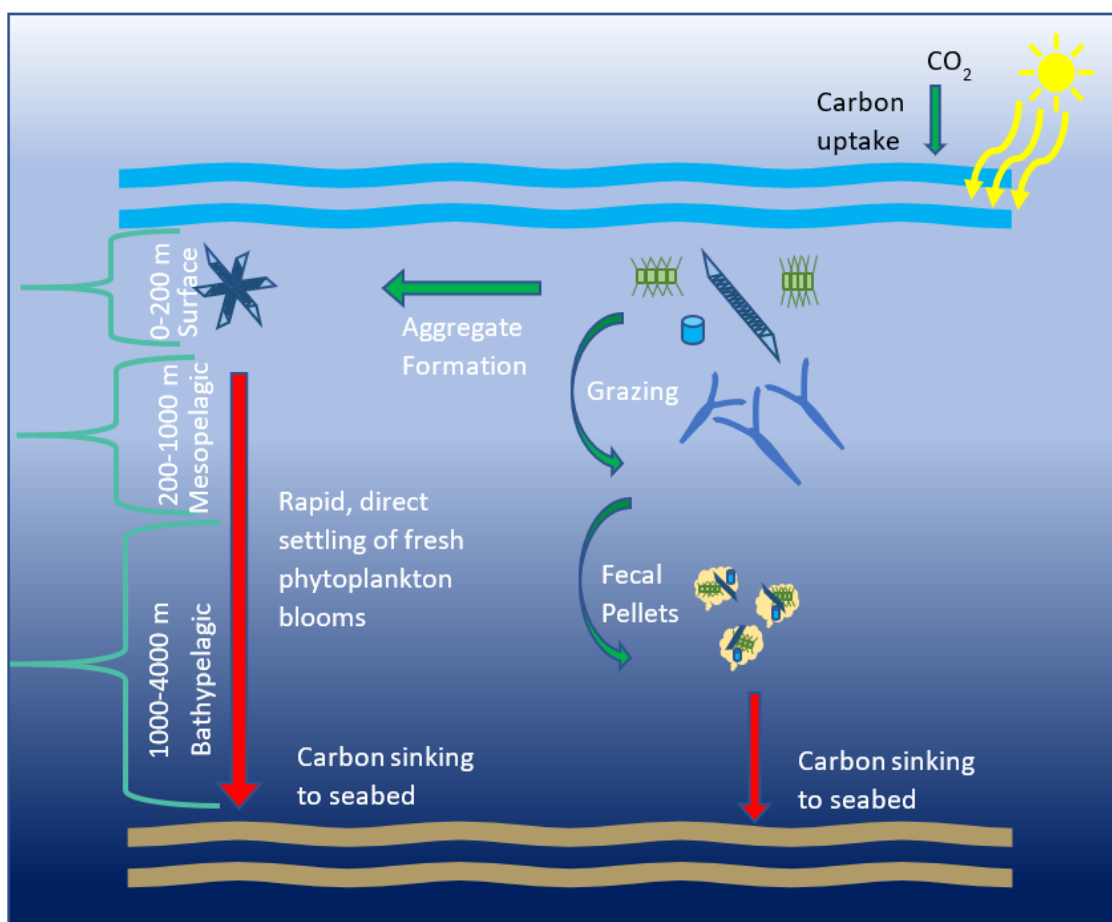


Figure 1. The biological pump in the ocean. Phytoplankton take up inorganic carbon from the surface of the ocean and fix it into organic carbon. The phytoplankton sink to the deep ocean by physical mixing, aggregate formation, or through fecal pellets. These sinking particles bring the organic carbon down to depth where benthic organisms can use this carbon as a source of food.

zooplankton. If the resulting aggregates and fecal pellets sink, they transport carbon to the mesopelagic where they encounter midwater food webs (Figure 1). This carbon would then sink to bathypelagic depths where long-term carbon sequestration occurs. We consider three possible mechanisms. First, if the particles sink very rapidly from the surface ocean, fresh phytodetritus may escape mesopelagic grazers and contribute to bathypelagic POC flux (Thiel et al., 1988). Second, the surface ocean particles can be grazed by surface zooplankton whose rapidly sinking fecal pellets may also reach the deep ocean (Ducklow et al., 2001). Third, sinking particles can be repackaged into fecal pellets and transformed by mesopelagic and bathypelagic food webs which generate the export of highly processed material to the deep ocean. It is important to distinguish between the three mechanisms because it would allow us to understand long-term changes in POC and help improve models of the ocean's carbon cycle.

Long term oceanographic timeseries stations such as Station ALOHA, Ocean Flux Program (OFP), Porcupine Abyssal Plain (PAP), and Station M have been measuring the export of carbon to the deep ocean for more than 30 years. Station ALOHA is a subtropical open ocean site located north of Hawaii ($22^{\circ} 45' N$, $158^{\circ} W$) and carbon export is measured in the bathypelagic as a way to complement primary production measured at the surface along with export measurements in the mesopelagic zone (Karl et al., 2012). Most of the particles that reach bathypelagic depths are highly processed by the midwater food webs. The episodic high pulses of POC measured at ALOHA were predominantly made up of fresh, unprocessed, diatom cells. The chemical measurements of nitrogen isotopes (Karl et al. 2012) suggested that the carbon was relatively fresh and was produced by diatoms. This indicates that high-flux events in this subtropical location are generated by rapid transport of fresh phytodetritus from the surface ocean to the deep sediment traps, bypassing mesopelagic food webs. A second long-term oceanographic timeseries station, OFP (Ocean Flux Program), is located in the western gyre of the Sargasso sea, southeast of Bermuda (Conte et al., 2001). There is a 30-year record of particle fluxes at 3200m depth (Conte et al., 2001). Most of the POC fluxes occurring are very low, but these fluxes are episodically enhanced by mesopelagic food webs when surface supply increases. There are almost no fresh, intact cells detected in these enhanced flux periods suggesting that the particles went through more processing

steps as they were sinking and that mesopelagic food webs play an important role in mediating the flux pathway. Neither of these studies directly observed the particle contents with microscopy.

Station M is a long-term oceanographic timeseries located in the Northeast Pacific ($34^{\circ}50'N$, $123^{\circ}00'W$, 4000 m deep) (Smith & Druffel, 1998), which differs from both Station ALOHA and OFP because it is within an upwelling region that is influenced by coastal currents and high primary production in the area. Station M also has more variable POC fluxes compared to these two subtropical locations. Large episodic pulses of particulate organic carbon (POC) sinking to the sea floor have been documented for 30 years (Smith et al., 2018). The occurrence of large episodic pulses is an important process because it has contributed to a long-term increase of carbon export to this deep ocean location and accounts for 25-63% of the total carbon that reaches the seafloor annually (Smith et al., 2018, Figure 2). It is unknown whether high-flux events are caused by the direct transport of fresh phytodetritus, surface produced fecal pellets, or processed by

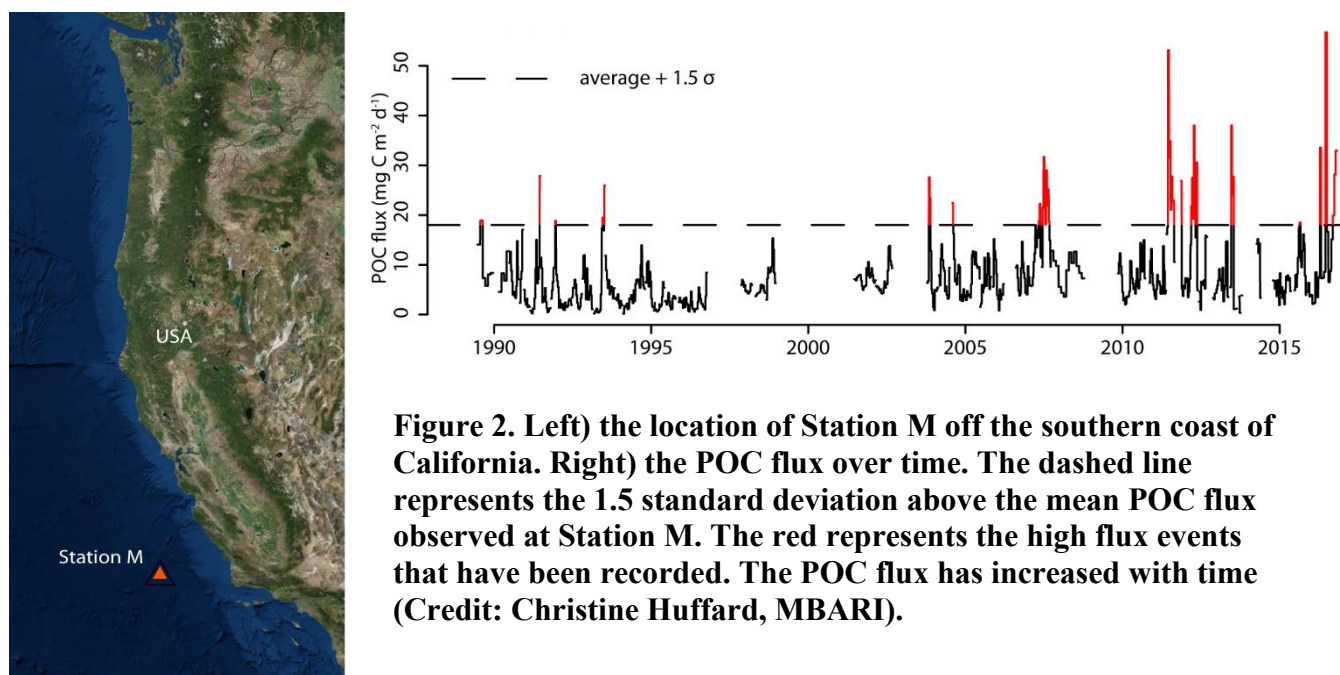


Figure 2. Left) the location of Station M off the southern coast of California. Right) the POC flux over time. The dashed line represents the 1.5 standard deviation above the mean POC flux observed at Station M. The red represents the high flux events that have been recorded. The POC flux has increased with time (Credit: Christine Huffard, MBARI).

grazing and repackaged into fecal pellets in the mesopelagic. These questions can be addressed by a detailed look at the phytoplankton cells within particles using microscopy

to directly observe the cells, along with biomineral analysis to help understand the mechanisms driving high POC fluxes at Station M.

Several environmental and climatological processes are known to influence the magnitude of POC flux at Station M. Upwelling within the California Current System brings nutrient rich waters to the surface, stimulating primary productivity and fueling new production by phytoplankton blooms (Smith, et al., 2013). Increases in upwelling have been observed and are caused by climatological changes in atmospheric pressure gradients (Bakun et al., 2015). Increased upwelling and nutrient supply could enable more phytoplankton to bloom off the coast of California and also advect more coastal phytoplankton communities offshore (Bakun et al., 2015). In a 15-year time series, Kahru et al. (2012) found that chlorophyll concentrations have increased along the central California coast. Low productivity was observed in the subtropical gyre due to increased stratification and lower nutrient fluxes, while higher productivity was observed along the central California coast (~0 -1000 km) due to increased upwelling. Higher productivity increases the amount of coastal phytoplankton communities that have the potential to sink and contribute to deep ocean carbon supply. Smith et al. (2013) identified a correlation between surface primary production and POC export at Station M. A time lag of approximately 10 days (Smith et al., 2018) signified that the carbon produced by surface production is quickly transferred from the surface to the bathypelagic. It is unknown whether those particles sink directly through the water column or are further processed and repacked by epipelagic and mesopelagic food webs before reaching bathypelagic depths.

At smaller spatial scales, ocean fronts in the California Current are areas in which enhanced POC export occurs from the surface into the mesopelagic. The enhanced export is due to subduction of the surface water in these areas and a greater amount of mesozooplankton biomass, allowing for more grazing to occur at these front regions (Stukel et al., 2017). This increased export would cause the phytoplankton communities transported offshore to sink more rapidly, contributing to the greater total export of POC. However, it is currently unknown whether particles transported into the mesopelagic by this mechanism continue to efficiently export carbon into the bathypelagic.

It is very difficult to directly link events through 4000 m of water, due to the physical dynamics and complex ecological interactions that are occurring in the water column as particles sink. However, the contents of the particles can help us narrow down which mechanisms might be most important. Phytoplankton community composition, cell size, cell fragmentation, and biomineral content can reveal the original source of the POC and the relative importance of zooplankton grazing versus direct export of rapidly sinking cells (through aggregation or ballasting) in generating these high-flux events. By using phytoplankton cells as indicators for different mechanisms, we can determine whether there was a rapid sink of fresh phytoplankton cells or whether there was enhanced processing of fluxes in the epipelagic or mesopelagic.

Different phytoplankton communities are associated with POC produced in offshore versus coastal environments, which can help indicate the original source of POC reaching bathypelagic depths. The types of phytoplankton blooming in the region of increased upwelling have been documented by the California Cooperative Oceanic Fisheries Investigation (CalCOFI). CalCOFI assessed the biomass of different types of phytoplankton in coastal communities compared to offshore communities. Coastal communities of phytoplankton are primarily composed of diatoms, while offshore communities were numerically dominated by coccolithophores (Venrick, 2015). Since coastal communities are composed primarily of diatoms, those communities being transported offshore by upwelling and lateral advection would most likely primarily contain diatom cells. Increased primary production could result in greater aggregate formations or zooplankton grazing. This would lead to a large quantity of phytoplankton-derived carbon and their remnants within sinking particles. If high-flux events are derived from coastal blooms, we would expect them to be enriched in diatoms or the remains of diatoms.

Large diatom cells can have physiological adaptations that make them more likely to reach bathypelagic depths than small cells. For example, Villareal et al. (1996) observed the vertical migration of *Rhizosolenia*. These cells form mats and migrate which enhances their downward movement. Another mechanism that could lead to direct transport of POC would be through aggregates of large diatoms. These aggregates are formed by large, slow-growing diatoms that live in low light intensities (Kemp et al.,

2000). These large diatoms grow slowly at low light levels in the water column to obtain nutrients. At the end of the summer season when more turbulence occurs, these large diatoms are mixed up through the water column to high light intensities. The diatoms are no longer in their ideal growing situation and become stressed, which causes them to produce carbohydrates causing the cells to stick to each other. The cells will form aggregates and start to sink through the water column. Kemp et al. (2000) found that large diatom aggregations become more abundant when fall/winter mixing breaks down the stratification in the ocean and called this process the 'Fall dump'. A similar process could occur during upwelling events, generating high fluxes of particles that contain larger diatom cells and their carbon. This mechanism would be consistent with a rapid influx of particles, along with the expectation that the large diatoms would be intact when they reach the sediment traps.

There is an entire ecosystem between the surface and the bathypelagic that particles transit through. During the transit, the particles could either be attenuated by microbial activity or be repackaged by zooplankton grazing. If grazing enhances POC flux, then sinking particles would contain more fragmented and empty cells. Conte et al. (2001) hypothesized that grazing by zooplankton could be stimulated by the rapid sinking of particles from the surface. Since it was found that the time lag between surface primary production and POC flux at Station M (4000m) is ~10 days (Smith et al., 2018), the particles are sinking rapidly. This rapid influx of particles from the surface water would allow the zooplankton in the mesopelagic to increase their grazing rate and allow for highly processed particles to be transported down to the bathypelagic sediment traps. Quantifying the degradation of phytoplankton cells collected in the sediment traps can therefore help determine what mechanisms are causing high POC flux events to occur at Station M.

Another important factor that can increase export of carbon is the ballasting due to biomineralization including biogenic silica (BSi), or opal-A, and particulate inorganic carbon (PIC), or calcium carbonate, produced by phytoplankton cells. Biominerals are denser than seawater making particles sink relatively rapidly (Armstrong, et al., 2002). BSi is primarily precipitated by diatoms and rhizaria while calcium carbonate is primarily precipitated by coccolithophores and foraminifera. When the cells die or are incorporated

into sinking particles, their biominerals are also incorporated into sinking particles. These biominerals make the particles denser and faster sinking and potentially increase POC flux, a mechanism referred to as the ballast hypothesis (Klaas & Archer, 2002). If this hypothesis is correct, then more biominerals (i.e. biogenic silica and calcium carbonate) within sinking particles could be driving the large POC fluxes to the deep ocean. Within the upper 100 meters of the water column, 50-60% of the biogenic silica produced in the euphotic zone is dissolved on average (Van Cappellen et al., 2002) as diatoms sink. Therefore, areas in the ocean where BSi production is higher and can still escape dissolution are important when discussing the ballast hypothesis. In high latitude areas such as the North Atlantic 60% of the POC flux is associated with the ballasting of minerals (Le Moigne et al., 2014). In the Southern Ocean the percentage drops to around 40% (Le Moigne et al., 2014). Today as much as 50% of the carbon export to the deep ocean is made up of siliceous phytoplankton, including diatoms (Ragueneau et al., 1996). Iron limitation of surface phytoplankton may also be important is the silica content of sinking particles. Less iron in waters induces diatom cells to uptake more silicic acid and become highly silicified, potentially enabling them to transport more carbon down to the mesopelagic (Krause et al., 2015). The California Current has low iron available (Hutchins & Bruland, 1998), inducing the diatoms to uptake more silica near Station M. It is important to consider biomineralization in this environment because the diatom cells are potentially more silicified than in iron-replete ecosystems. Importantly, ballasting may enable particles sinking from the upper ocean to sink fast enough to evade processing by midwater food webs, including zooplankton grazing and bacterial degradation. This could affect the biomineral content of the particles and may reduce the effect of ballasting on the export of highly processed particles. If biomineral ballasting causes high POC flux events at Station M, we would expect to find larger numbers of diatom and coccolithophore cells (i.e. cells with harder skeletal parts) within particles sinking during high-flux events and a higher concentration of biominerals within exported particles. If biomineral ballasting is not associated with high POC flux events, we would expect there to be no difference or a reduction in both the mineralization and the concentration of diatom and coccolithophore cells in particles sinking during high-flux events compared to low-flux periods.

POC flux to the seafloor is increasing at Station M (Figure 2) in the California Current due to episodic high-flux events, but the ecological mechanisms causing this increase is unknown. The clue to the mechanism may be identified from the phytoplankton communities within particles sinking at Station M. The phytoplankton can be analyzed to help determine if the mechanism was a direct export of fresh particles from the surface (i.e. intact cells), or if there was enhanced processing in the mesopelagic (i.e. fragmented cells). Detecting the mechanisms driving POC flux events at Station M might be pertinent for other highly productive eastern boundary currents in the world. Station M is a unique location along an eastern boundary current compared to other long-term open ocean station that have been collecting POC flux data. The evidence that increased POC flux has a positive correlation with increased biomineral flux in open ocean settings potentially indicates that biomineral fluxes could influence the total carbon sequestration. By resolving the effects of phytoplankton and biominerals on the POC fluxes we will be better able to determine the mechanisms involved in high-flux events.

Some questions to address in this study are: 1) Do particles sinking during high POC flux events contain greater quantities of phytoplankton cells? 2) Does ballasting of sinking particles by biominerals cause high flux events? The first question can be answered by the first hypothesis, high-flux events at Station M are caused by direct export of fresh phytodetritus to abyssal depths that avoid the processing mechanisms in the epipelagic and mesopelagic. This can be addressed by looking at the phytoplankton cells within the sinking particles to see how processed the cells are. The less processed the cells the more likely the cells avoided enhanced mesopelagic food webs and were rapidly sinking. The more processed and fragmented the cells the more likely that zooplankton grazing and bacterial degradation occurred as the particles sank. The second question can be answered by the second hypothesis, high-flux events at Station M are caused by ballasting of sinking particles with biogenic silica and calcium carbonate. This hypothesis can be addressed by measuring the biominerals within the particles that are attributed to ballasting (i.e. biogenic silica and PIC). Higher amounts of ballasting minerals within high-flux events would support the ballast hypothesis suggesting that denser particles will sink more rapidly. Less biominerals within the high-flux events would not support the ballast hypothesis.

METHODS

SAMPLES COLLECTED

Samples were collected off coastal California at Station M (34°50'N, 123°00'W, 4000 m deep) in McLane Parflux Mark 78H2 (Smith et al., 2013) sediment traps deployed 600 meters above the sea floor (Smith et al., 2018). The sediment traps have large funnel shaped openings that collect the sinking particles into different cups. The 21 cups are arranged on a carousel that rotates to the next cup every 10 or 17 days. Several samples were lost during this time series due to the cups clogging and blocking particles from entering the cup. Samples were collected by K.L. Smith starting in 1989 until present day and the samples selected for this study correspond with periods of high carbon flux measured in the sediment traps (Smith et al., 2018). The high-flux events are defined as fluxes greater than 1.5 times the standard deviation of the average flux of all the samples collected (Smith et al., 2018). In order to determine whether the particles sinking during high-flux events contain a different phytoplankton community and different amounts of biominerals, high-flux samples were compared to samples collected immediately before and after each high-flux event (hereafter referred to as low-flux periods). These two types of samples were used to determine whether changes in community composition or biomineral content within particles were associated with the large increase in the amount of carbon sinking to depth during high flux events.

PIC and POC were previously measured in each of the samples as part of the Station M time-series program (Smith et al., 2018). PIC is the mineral found in coccolithophores and foraminifera (calcium carbonate). POC is the total amount of organic carbon collected in the sediment trap. POC is present in all organisms and also in sinking detritus. The total carbon was measured using an Elmer or Exeter Analytical elemental analyzer at the University of California Santa Barbara Marine Science Institute Analytical Lab. Inorganic carbon was determined using an UIC coulometer and a salt correction was performed by using AgNO₃ titration. The PIC was subtracted from the total carbon to calculate the total POC in the samples. The salt was subtracted from the sample weight in order to get the correct weight for the calculations of carbon flux. The

mass flux of PIC was then multiplied by 8.33 to calculate the mass flux of CaCO_3 (Lamborg et al., 2008). The full methods for the POC and PIC flux calculation can be found in the SI Appendix in Smith et al (2018).

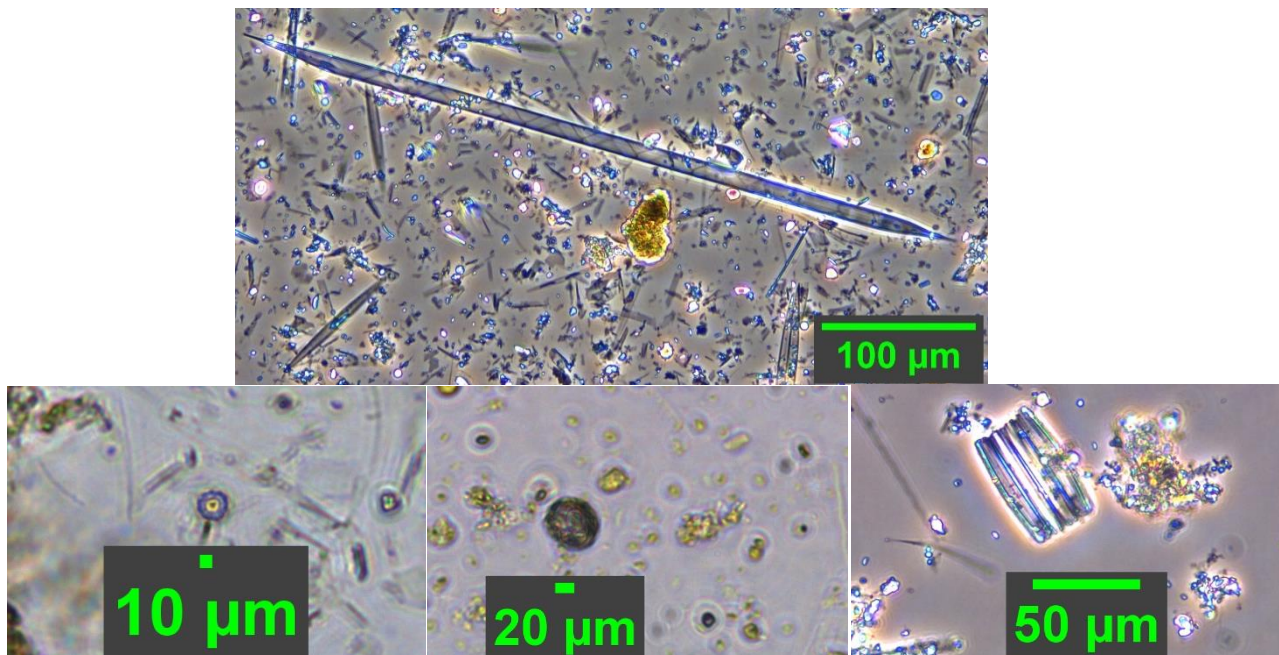


Figure 3. Example micrographs of cells. Top diatom *Rhizosolenia*, bottom left coccolithophore *Emiliana-like*, bottom middle coccolithophore *Coccolithus-like*, bottom right diatom *Fragilariopsis doliolus*.

MICROSCOPY

Microscopy was used to determine whether the phytoplankton composition within sinking particles changed during high-flux events. Samples were counted on an inverted Nikon Eclipse Ts2 microscope. The samples were diluted to distinguish different cells and avoid over-crowding the slide with detritus. Cells within a known fraction of 1 milliliter of the diluted sample were counted using a Sedgewick rafter (Figure 3). In order to ensure that a representative composition of species was detected, 2 nonparametric estimators of species richness were used to predict the theoretical number of species present within the sample after counting 400 cells (Chao et al., 2009). Cells were counted until at least 80% of the predicted cell types present were identified or until 1000 cells

were counted to permit timely analysis of all samples. To calculate the cell number fluxes, the cell count of the diluted sample was divided by the number of squares counted and then multiplied by the volume used to calculate the original concentration of the 1/8 subsample. Each trap sample was previously split among 8 different collection tubes, so the volume of each split was multiplied by 8 to calculate total flux per trap sample. Finally, the volume-normalized cell abundances were divided by the number of days the cup was open (10 or 17 days) and the trap collection area (0.5 m²) to calculate cell number flux.

Cell Classification

Because cells were often fragmented or missing defining features, cells were classified by species, genus, or morphotype (hereafter referred to as cell type). The cells were classified as close to species as possible or otherwise the genus was recorded. If the genus could not be determined cells were instead categorized into broader morphological groups. For example, centric diatoms that could not confidently be named according to their genus were instead categorized by their corresponding size (small <50 μm, medium 50 μm -100 μm, large >100 μm). Some diatoms like *Chaetoceros* were combined into a single *Chaetoceros* group instead of grouping them based on species. The coccolithophores were assigned genus names, but they are possibly a combination of multiple morphologically similar genera. For example, the cells classified as *Emiliana*-like may include some *Gephyrocapsa* cells due to similar sizes and the poor resolution of their morphological differences by these methods. The goal in the categorization was to be as detailed in assigning cell names as possible without placing the cell into an incorrect category. The fragmented cells were also included in counts if the fragments were easily recognized and could be placed in a cell type category. Empty cells, cells that did not contain a chloroplast, were counted as well but were recorded distinctly from those cells that contained chlorophyll. Fragments and empty cells were only classified for diatom categories. The coccolithophores were only counted as whole cells because the light microscope could not resolve individual coccoliths.

CELL FLUX FROM PHYTOPLANKTON CELLS

A collection of micrographs captured from a subset of cells were used to model the carbon content in the cells. The maximum potential carbon derived from phytoplankton cells in the samples was modeled using the relationship between carbon content and volume of phytoplankton cells determined by Menden-Deuer & Lessard (2000).

$$\text{Diatoms: pgC cell}^{-1} = 0.288 * V^{0.811} \quad (1)$$

$$\text{Other Protists: pgC cell}^{-1} = 0.216 * V^{0.939} \quad (2)$$

The volume (V , μm^3) of the cells was calculated by measuring the pixel dimensions of a subset of representative cells using ImageJ software. The measure tool was used to measure the pixel dimensions of the representative cells. The pixel lengths were converted to microns and used to calculate the cell volume. Volume equations such as the equations for a cylinder and a sphere were used to estimate the cell's volume. Once the volume of a cell was calculated the value was used in equations (1), for diatom cells, and (2), for every other cell, to calculate the amount of carbon per cell. The carbon per cell was then multiplied by the cell number fluxes to model the cell carbon flux. This modeled cell POC flux was divided by the measured bulk POC flux collected in each of the traps to determine the fraction that each cell category contributed to total carbon flux. The second equation above was not developed specifically for coccolithophores, but since there is no equation specified for coccolithophores, we used this equation as an estimate to help draw further conclusions in the cellular carbon flux. Also, this equation was developed for living cells, and since many of the cells in the sediment traps were degraded and fragmented this calculation is an overestimate of the cellular contents of the entire community within the particles. For this reason, the modeled carbon flux is considered to be the maximum potential carbon flux by phytoplankton and is used to account for the different influence of cells with vastly different sizes, which are not apparent by analysis of number fluxes.

BIOGENIC SILICA

Biogenic silica contents of sediment trap samples were measured using the protocol by Strickland and Parsons (1972). Biogenic silica within the samples was dissolved in a strong base (NaOH) in a hot water bath followed by the addition of ammonium molybdate. Ammonium molybdate changes the absorbance of the solution in proportion to the concentration of silicic acid. Samples with a higher absorbance contain more silicic acid. In order to determine the amount of silicic acid dissolved in the sample, the absorbance of blue 810nm wavelength relative to a series of silicic acid standard solutions was measured using an Ocean Optics spectrophotometer (model: FLAME-S-XRI-ES). The standard solutions were made using a stock silicic acid mixed with water to dilute the silicic acid. The standards ranged from 0 μ M – 100 μ M. In order to determine the optimal incubation time required to dissolve the biogenic silica in the strong NaOH solution, two samples were incubated in the basic solution for increasing time intervals (0.5, 1, 2, 4, and 6 hours) (Figure 4). The BSi detected in the first sample was between 0.25 \pm 0.017 and 0.35 \pm 0.017 mg m⁻² day⁻¹ for the first 4 hours and increased to 0.425 \pm 0.017 mg m⁻² day⁻¹ after 6 hours. The BSi detected in the second sample remained relatively constant for all 6 hours, varying between 3 \pm 0.07 and 3.8 \pm 0.07 mg m⁻² day⁻¹. Since there was only one sample used for each time period, the errors calculated represent precision limits of the instrument (0.01 AU). This value was converted from AU to mg m⁻²d⁻¹ to determine the uncertainty of the instrument used in the time trials. When triplicate subsamples were incubated for 1 hour in the NaOH solution on average, the mean standard deviations were 16.7% average values. This range of error could have occurred from stochastic pipetting of the sample contents. This indicates that the time trial values show no meaningful change over the incubation time period. Therefore, a 1-hour incubation time was chosen for all samples because it was enough time to dissolve all the biogenic silica in the sample without any apparent contamination from lithogenic silica. To account for any variation in the composition of pipetted material, triplicate subsamples were measured from each sample. Some samples were below the level of detection (the absorbance was negative once corrected with the reagent blank), so these values were interpreted as zero for the purpose of this analysis. The lowest detected absorbance was 0.06AU which translated to -0.15 μ mol BSi m⁻²d⁻¹ (Supplementary

material Table 3). Only 5 samples out of 57 were below the level of detection.

Absorbance measurements were converted to biogenic silica by dividing the absorbance by the slope of the standards. This value was then corrected for the dilution and the filter blank and converted from $\mu\text{moles L}^{-1}$ to milligrams L^{-1} using the atomic mass of silicon. This value was multiplied by the volume of each sample, multiplied by 8 to account for

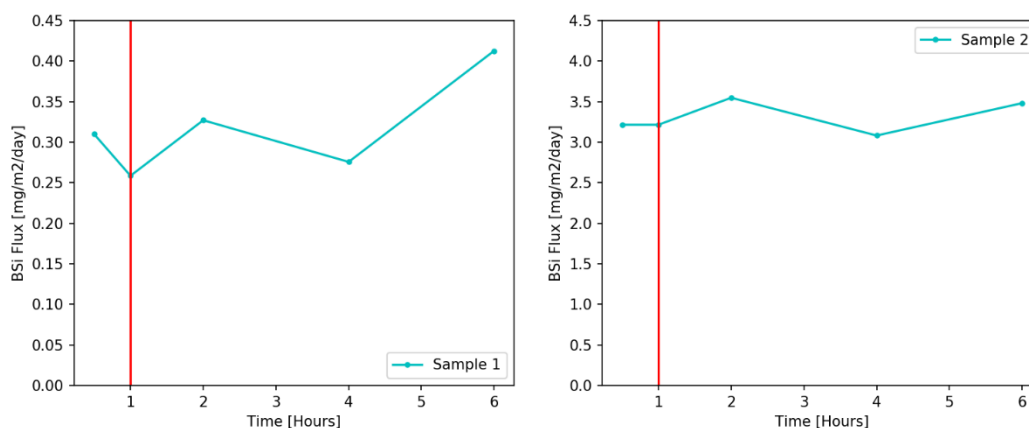


Figure 4. Time series incubation of two sediment trap samples in NaOH to determine the amount of time required to dissolve biogenic silica without lithogenic silica contamination. The red line represents the 1-hour period which was chosen for the method.

the 8 splits of the original trap sample, and then divided by the collection time and area of the trap to calculate the BSi flux. The BSi flux was then multiplied by 2.4 to calculate the opal flux (Lamborg et al., 2008). These data were then normalized to POC and compared to the PIC normalized to POC. Data were assessed to identify whether more biogenic silica (i.e. diatoms) and/or PIC (i.e. coccolithophores) were present within sinking particles during high-flux events.

STATISTICAL ANALYSIS

To test whether community compositions within sinking particles differed between high-flux events and low-flux periods (Hypothesis 1), a Bray-Curtis dissimilarity test was used as a comparison metric. This metric calculates the relative differences between communities to determine which samples are more similar. A multidimensional scaling (MDS) plot was used to visualize the Bray-Curtis dissimilarities

among all samples. The MDS plot helps to visualize which groups of samples are more similar based on their relative location in space to one another. A permutational multivariate analysis of variance (PERMANOVA) was used to assess the statistical significance between the communities present within high- and low-flux samples. The PERMANOVA tests whether two groups are different based on the average distance within a group compared to the distance between groups. We defined a p-value <0.01 as a significant difference and used this significance level for all statistical tests. The Bray-Curtis dissimilarity was calculated first on the entire community of intact cells, and then again on only the diatom community to compare the intact and fragmented cells. A SIMPER (similarity percentage) analysis was used to determine which cell types were most responsible for dissimilarity among samples. The SIMPER analysis is done on the Bray-Curtis dissimilarity matrix and uses a pairwise comparison on each of the samples to each other. It determines the percentage of the cell types that are causing the dissimilarity within the Bray-Curtis matrix.

To compare the relative contribution of phytoplankton to POC flux between high-flux events and low-flux periods, the following ratios were calculated for each sample; 1) cell number flux: measured POC flux and 2) modeled cell POC flux: measured POC flux. Because these data were not normally distributed, differences between high-flux periods versus low-flux periods were tested using a Mann-Whitney test. The Mann-Whitney test is a nonparametric statistic that tests whether the median (i.e. normalized cell flux) from a group of samples is higher or lower than the median in the other group of samples. If a p-value of <0.01 was found, the sample types were considered different from each other. These analyses were performed separately for each major phytoplankton functional group (intact diatoms, fragmented diatoms, nanoflagellates, and coccolithophores). Cell species with less than 5 cells counted in a sample were grouped into an 'other diatom', 'other coccolithophore', or 'other protist' category due to a high counting uncertainty. This grouping was used to look at the individual types of phytoplankton driving differences in the high-flux events. The normalized flux of intact diatoms (containing chloroplasts) was compared to the normalized flux of fragmented diatom cells (without chloroplasts) between samples collected during high-flux events and low-flux periods using a Mann-

Whitney test. This was used to test whether particles were more enriched in chlorophyll containing diatoms during high POC flux events or the low-flux periods.

The diversity of the intact communities sinking within particles during high-flux versus low-flux periods was calculated using a Shannon diversity index. The Shannon diversity index relates the number of different species within a sample to the observed abundance of each species in a sample. The average Shannon diversity index was calculated for the high POC flux samples and low-flux periods. A higher index indicates greater diversity within that group. A t-test was used to determine if the means of the two indices were different from each other by using the $p\text{-value} < 0.01$ to determine a significant difference.

The relationship between biomineral fluxes (opal and CaCO_3) and POC fluxes were assessed by linear correlation (Hypothesis 2). Next the opal and CaCO_3 were normalized to the total POC calculated for each sample. This normalization (opal: POC and CaCO_3 : POC) allowed for the high-flux and low-flux samples to be compared to determine if the high-flux events were more enriched in biominerals per unit POC. A linear correlation analysis was calculated to assess the relationship between the normalized opal and CaCO_3 to total POC. Differences between the median normalized biomineral content during high-flux events versus low-flux periods were analyzed using the above described Mann-Whitney test and were considered statistically significant at $p\text{-value} < 0.01$.

We further quantified variability in the biological characteristics among individual high-flux events. For each event, measurements collected from particles sinking during the event were divided by measurements collected from particles sinking before or after the event. A ratio < 0.5 was considered to be a substantial decrease in the measure during the event compared to the samples before or after the event. A ratio > 2 was considered to be a substantial increase in the measure during the event compared to the samples before or after the event.

RESULTS

Phytoplankton community composition within sinking particles were assessed to provide an indication of the mechanisms causing high POC flux events. High POC flux events at Station M are causing the long-term increase in POC (Smith et al., 2018)

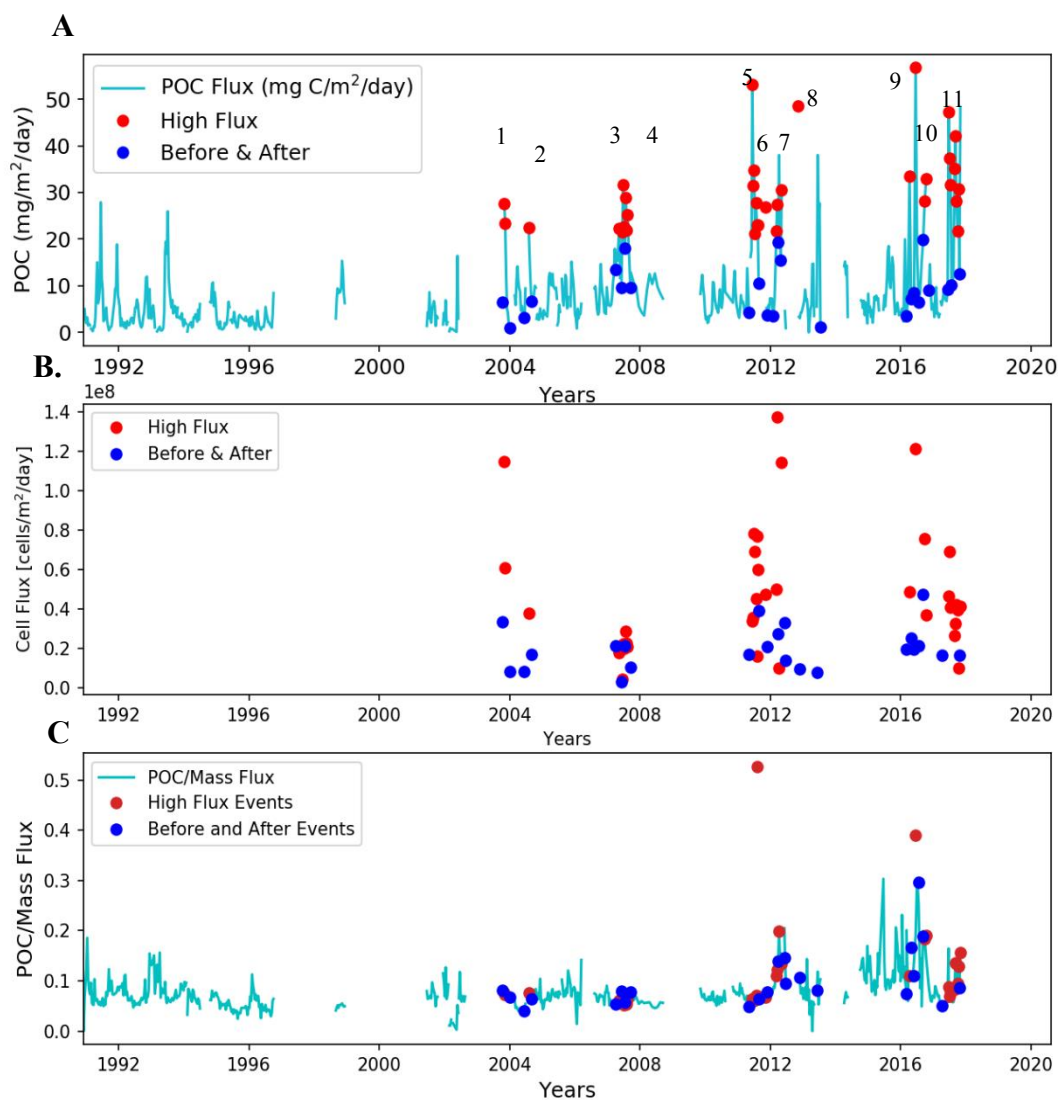


Figure 5. (A) The total carbon flux over the entire time series (blue line). The red dots indicate the high-flux event samples and the blue dots indicate the low-flux samples. The numbers represent the event number for the high-flux events. (B) The total cell flux in cell/m²/day over the time series. (C) The total POC normalized to mass flux over the entire time series. The red dots represent the high-flux events and the blue dots represent the low-flux periods.

(Figure 5). Carbon export and high-flux events have increased in frequency and magnitude over time (Smith et al., 2018, Figure 5A). The total cell number flux has followed the same trend with higher cell fluxes during high POC flux events (Figure 5B). The POC: mass flux (Figure 5C) shows that a majority of high POC flux events make up less than 50% of the total mass flux of sinking particles. The ratio of POC: mass flux was relatively constant $\sim 10\%$, which indicates the relative “freshness” of particles was not changing. If particles were less processed due to reduced grazing or remineralization, then the POC:mass flux would be higher. If the particles were more processed (i.e. nutritious parts consumed), then POC:mass flux would be lower. The most abundant functional groups identified in the samples were diatoms, coccolithophores, and nanoflagellates (Figure 6) and we focus our analysis on these most abundant groups.

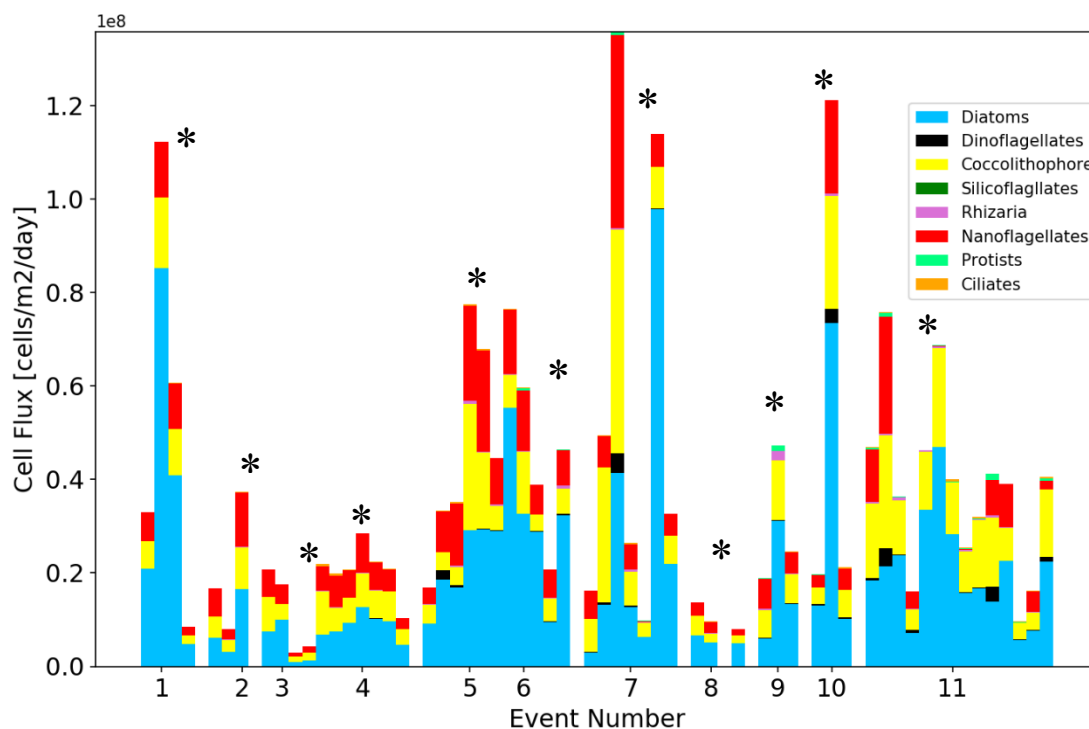


Figure 6. The identity of the different types of cells in each sample over the time series. The colors in the legend show the different types of cells and their flux in cells/m²/day in each sample examined. Asterisk represents high-flux events.

The three major phytoplankton groups that composed the majority of the number fluxes (diatoms, coccolithophores, and nanoflagellates) were individually examined to determine whether they were more enriched within particles collected during high-flux events. Diatoms were analyzed as both intact and fragmented, coccolithophores were considered intact (due to resolution of the microscope), and nanoflagellates were considered intact. This generic nanoflagellate category was potentially composed of small oocchrophytes and chlorophytes as well as heterotrophic protists that may be degrading organic matter as it is sinking to the deep ocean. The number flux of intact diatom cells relative to the total POC flux was compared between high-flux samples and low-flux periods. The relative number flux of intact diatom cells (containing chlorophyll) within particles was 3x smaller during the high-flux events than the before or after the

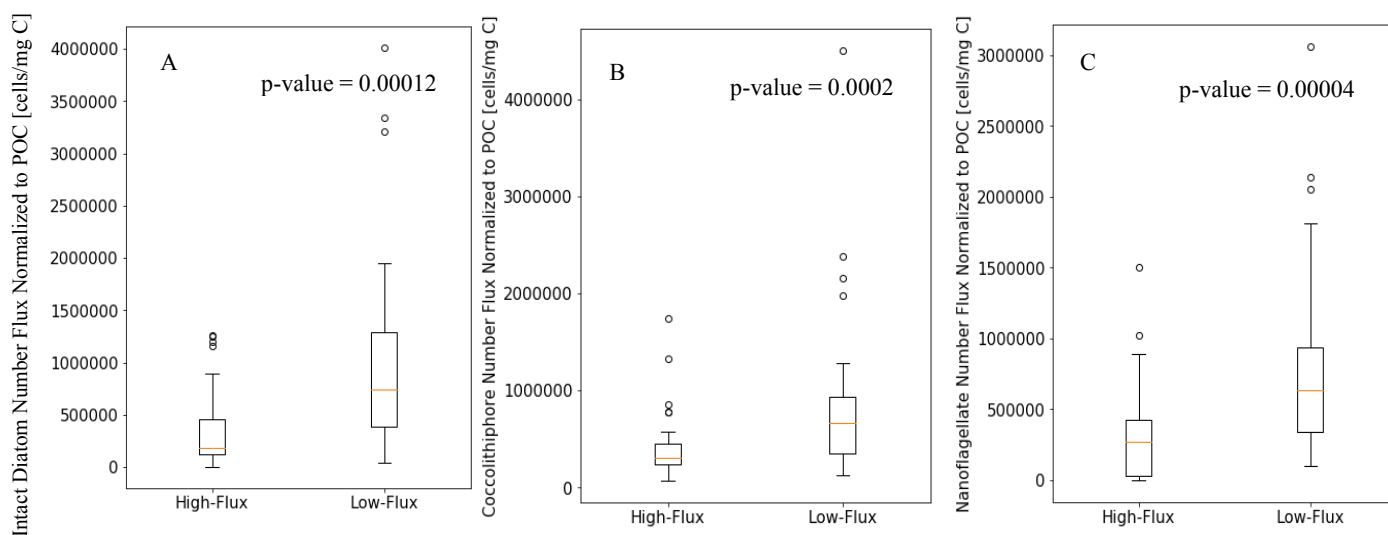


Figure 7. A) the relative number flux of intact diatoms; significantly fewer intact diatoms were seen in the high-flux events (p-value <0.001), B) the relative number flux of coccolithophores; significantly fewer coccolithophores were seen in the high-flux events (p-value <0.001), C) Nanoflagellate relative number flux; significantly fewer nanoflagellates were seen in the high-flux events (p-value <0.01).

event (p-value = 0.00012) (Figure 7A). The relative number flux of coccolithophore cells was 2.5x smaller in samples collected during high-flux events compared to samples collected during low-flux periods (p-value = 0.0002) (Figure 7B), similar to diatoms. The relative number flux of nanoflagellates was 3x lower during high-flux events compared to

the low-flux periods (p-value = 0.00004) (Figure 7C). Again, this is similar to the results for both the diatoms and coccolithophores.

To determine whether the cells' modeled maximum contribution to carbon flux changed between high-flux events and low-flux periods, the carbon flux of each functional group was modeled based on cell size and normalized to measured total POC flux. Intact diatoms accounted for 2.25x less of the carbon flux during high-flux events compared to low-flux periods (p-value = 0.002) (Figure 8A). This result is consistent with the diatom cell number fluxes where lower relative cell fluxes were observed during the high-flux periods for intact diatom cells. There are some values where intact diatom C:POC >1 which implies that there are errors in the carbon modeling which will be discussed in more detail. Changes in the relative carbon flux by coccolithophores also reflected the changes in relative cell flux with 2x lower relative coccolithophore carbon flux in samples collected during high-flux events compared to low-flux periods (p-value = 0.0008) (Figure 8B). The relative carbon flux by nanoflagellates was 3x lower during the high-flux events compared to low-flux periods (p-value = 0.00004) (Figure 8C). The relative number flux of diatoms was reduced at the onset of the high flux event in 38% of

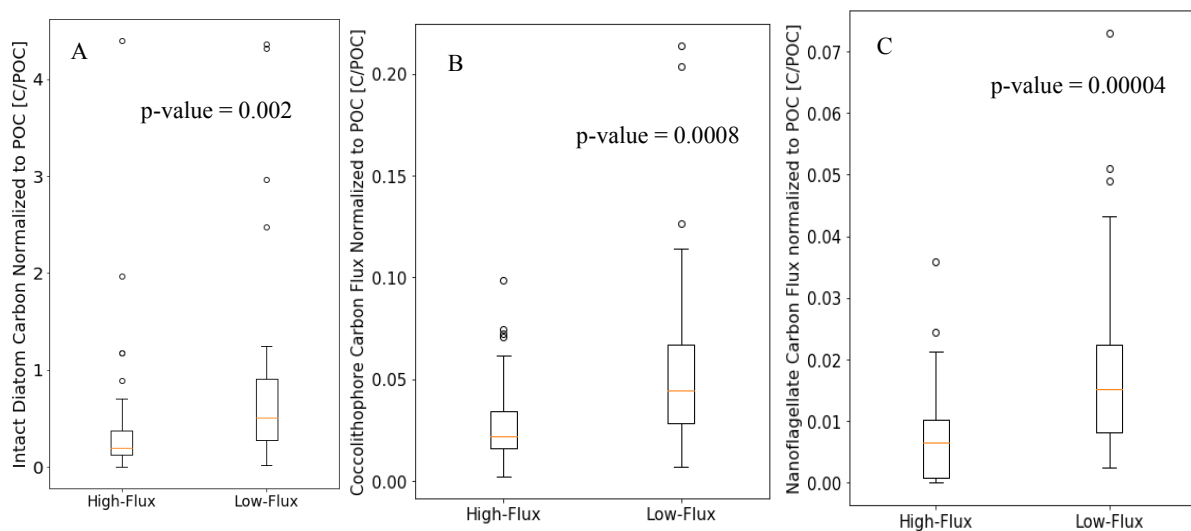


Figure 8. A) Intact diatom relative carbon flux; significantly less carbon was transported by intact diatoms during high-flux events B) coccolithophore relative carbon flux; significantly less carbon was transported by coccolithophores during high-flux events, C) nanoflagellate relative carbon flux; significantly less carbon was transported by nanoflagellates during the high-flux events.

the events and increased after 50% of the events (Table 1). This suggests that the diatom community contribution to flux was more likely to change after the high-flux event compared to at the onset of the event. The relative number flux of coccolithophore cells decreased at the onset of the event in 38% of the samples and increased again after the termination of the event in 50% of the samples. The relative number flux of nanoflagellates decreased at the onset of the high-flux events in 50% of the events and increased again after the event in 38% of the events. Table 1 shows the percentage and number of events of an increase or decrease of cell number flux at the onset or after the event.

The fragmented diatoms were analyzed separately from intact cells to identify clues to different mechanisms. Unlike intact cells, the relative number flux of fragmented

Table 1. The functional groups increasing or decreasing during or after the onset of the event								
Functional Group	Increased at Onset		Decreased at Onset		Increased Afterwards		Decreased Afterwards	
	Diatom	25%	2/8	37.5%	3/8	50%	4/8	12.5%
Coccolithophore	12.5%	1/8	37.5%	3/8	50%	4/8	0%	0/8
Nanoflagellate	25%	2/8	50%	4/8	37.5%	3/8	0%	0/8

and/or empty diatom frustules within particles was not significantly different between high-flux events and low-flux periods (p-value = 0.0213) (Figure 9A). There was no significant difference in modeled relative carbon flux by fragmented diatoms during high-flux events versus low-flux periods (p-value = 0.50) (Figure 9B), which agrees with the cell number flux for fragmented diatom cells. The ratio of modeled diatom carbon:total POC was sometimes greater than 1. The equation used to model the carbon was created based on healthy, live cultures and may not take into account the amount of degradation the cells sinking went through.

The influence of large-sized diatom cells on POC flux were assessed to determine whether their distinct life history and adaptations played a role in generating high-flux events. Large and small diatom cells' carbon flux was assessed relative to cell sizes and whether the cells were intact or fragmented. Those cells whose modeled carbon content was $<1000\text{pgC cell}^{-1}$ were categorized as small cells and those $> 1000\text{pgC cell}^{-1}$ were

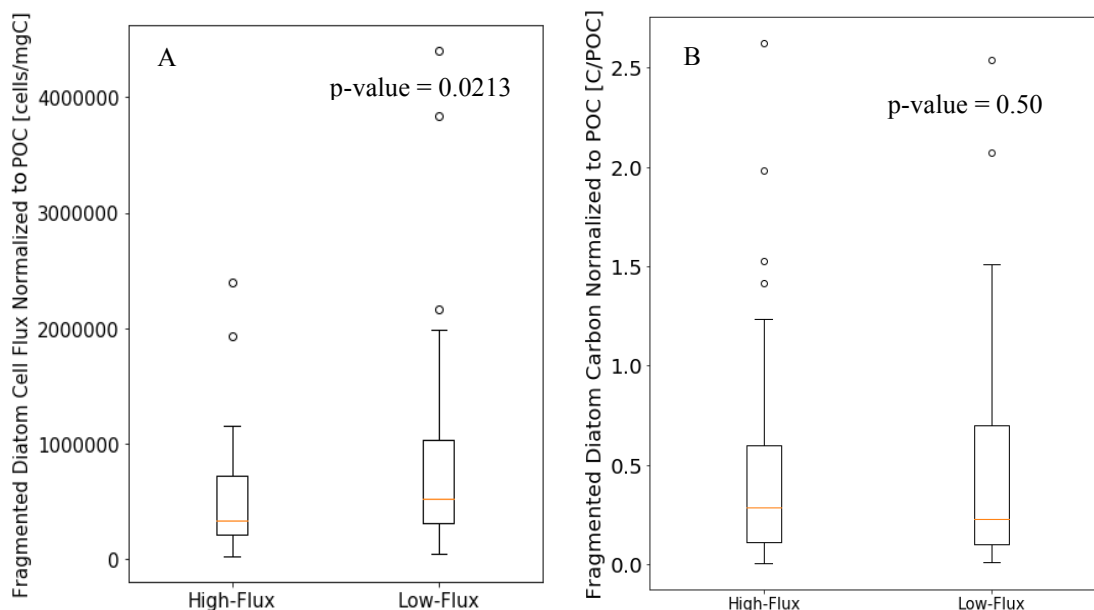


Figure 9. A) The relative number flux of fragmented diatoms; there was no significant difference between fragmented diatom number flux during high-flux events and low-flux periods. B) Fragmented diatom relative carbon flux; there was no significant difference between high-flux events and low-flux periods.

categorized as large cells. The modeled relative carbon flux by both size classes of cells containing chlorophyll was significantly lower during high-flux events (large cell p-value = 0.0082 small cell p-value = 0.004, Figure 10A). The modeled relative carbon flux did not change between the high-flux events compared to low-flux periods in fragmented large cells (p-value = 0.133) and fragmented small cells (p-value = 0.14) (Figure 10B). This is similar to the results with the previous relative carbon flux for live and fragmented cells.

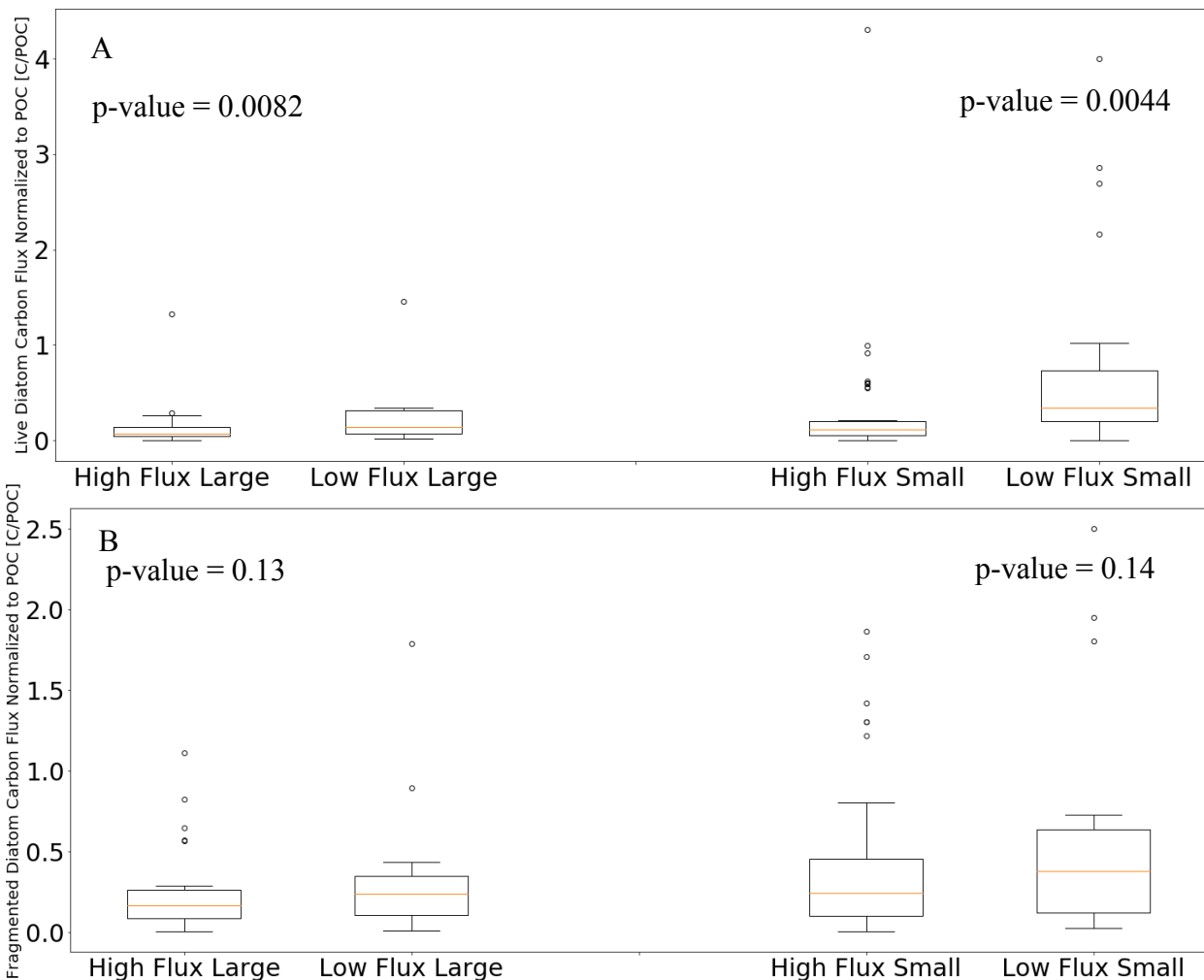


Figure 10. A) relative carbon flux for live diatom cells separated by size (large and small), B) relative carbon flux for fragmented diatom cells separated by size (large and small).

Although there seemed to be a uniform change in relative flux at the functional groups' classification level, the taxonomic composition within those groups also changed during high flux events. To identify changes in the community composition within sinking particles, a Bray-Curtis dissimilarity matrix was created to compare the communities of intact cells present within particles during high-flux events and low-flux periods. Particles sinking during these two time periods contained two distinct communities of intact phytoplankton (p-value = 0.001, PERMANOVA, Figure 11). A SIMPER analysis was used to determine which cell types were most responsible for

dissimilarity within all the intact cells. The higher the percentage of the cell type the more that cell influenced the dissimilarity in the Bray-Curtis dissimilarity matrix. *Emiliana* and *Pseudo-nitzschia* are responsible for >50% of the dissimilarity found in the Bray-Curtis matrix for intact cells in high- and low-flux events (Table 2). To determine whether the composition of fragmented diatoms differed from the composition of intact diatom cells, a second matrix of Bray-Curtis dissimilarities was calculated that compared all intact diatom communities with all fragmented diatom communities in all samples. The intact diatom communities present within the particles did not differ between high and low flux events (p-value = 0.032, PERMANOVA, Figure 12, top left). The fragmented diatom communities present within the particles did differ between the high-

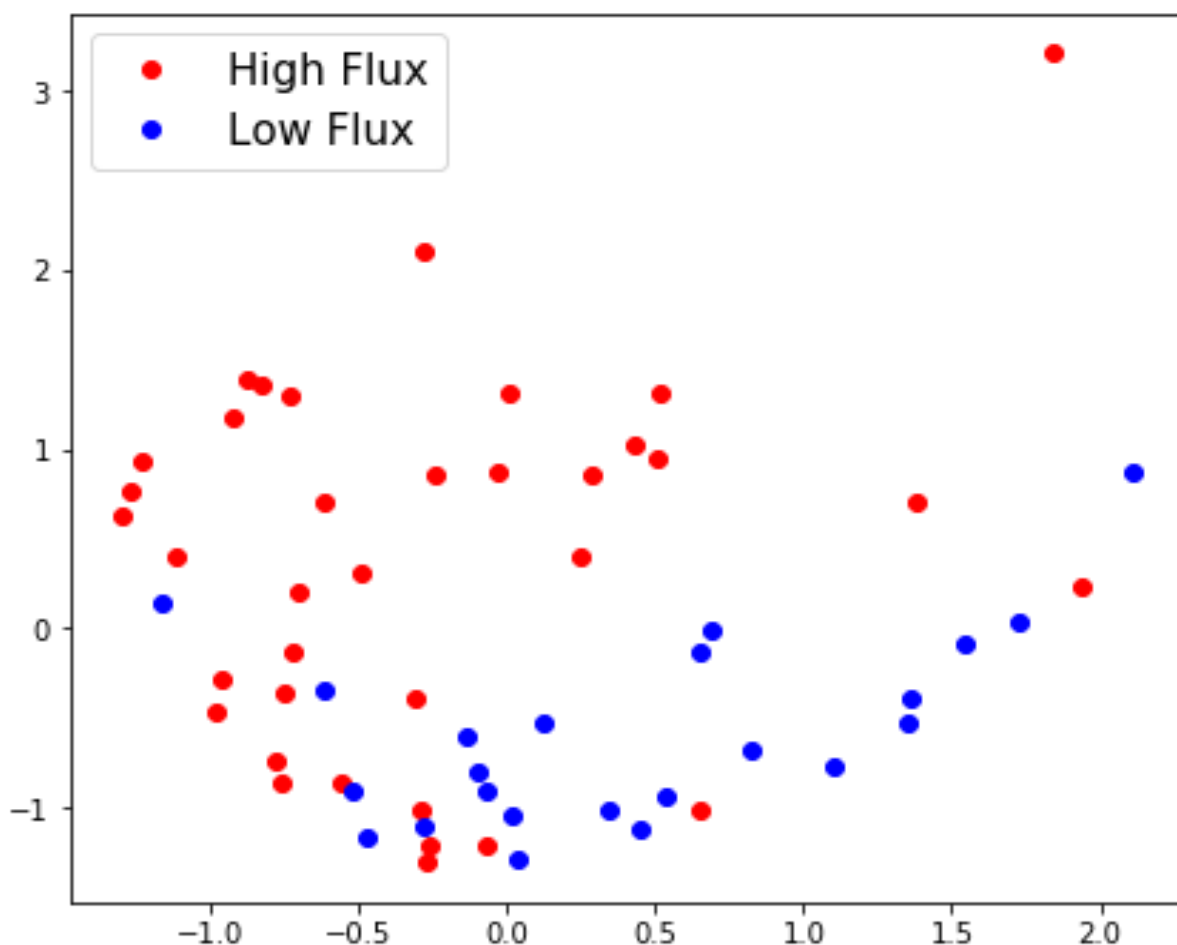


Figure 11. MDS plot of high flux (red) and low flux (blue) samples. Two significantly different clusters are plotted (p-value = 0.001).

and low-flux events (p-value = 0.001, PERMANOVA, Figure 12, top right). Next, the high-flux fragmented versus high-flux intact were analyzed to see how the community changed. There was no difference between high-flux fragmented and high-flux intact (p-value = 0.137, PERMANOVA, Figure 12, bottom left). The same analysis was done on low-flux fragmented and low-flux intact. Again, no difference was found (p-value = 0.216, PERMANOVA, Figure 12, bottom right). The PERMANOVA results indicate that the fragmented diatom cells were causing the difference between high- and low-flux events. Another SIMPER analysis was used to determine which cell types were most responsible for dissimilarity within the fragmented diatoms. The higher the percentage of the cell type the more that cell influenced the dissimilarity in the Bray-Curtis dissimilarity matrix. *Skeletonema*, *Chaetoceros*, and small *Nitzschia* cells were responsible for >50% of the dissimilarity in the Bray-Curtis dissimilarity matrix of fragmented diatom cells in the high- and low-flux events (Table 3). The difference in communities led us to investigate the diversity to see if one type of cell bloom could have been causing the difference between high- and low-flux events. To test if diversity was changing between high-flux events and low-flux periods, a Shannon diversity index was calculated for intact cells and was found to be 1.77 ± 0.51 during high-flux events and 1.90 ± 0.46 during low-flux periods. A p-value of 0.36 indicated that there was no significant difference between the diversity of the high- and low-flux events, despite the significant difference in community composition.

Cell Type	Percentage	Fold Change
<i>Emiliana</i>	45.56%	~2.4x lower in high-flux events
<i>Pseudo-nitzschia</i> large	13.66%	~3x lower in high-flux events
<i>Skeletonema</i>	4.8%	No fold change
<i>Helicosphaera</i>	4.12%	No fold change
Medium centrics	3.65%	~2x lower in high-flux events
<i>Coccolithus</i>	3.54%	~2.5x lower in high-flux events
<i>Chaetoceros</i>	2.62%	~3x lower in high-flux events

Table 3. SIMPER analysis results of fragmented diatom cell types that determine dissimilarity		
Cell Type	Percentage	Fold Change
<i>Skeletonema</i>	36.38%	No fold change
<i>Chaetoceros</i>	10.24%	No fold change
Small <i>Nitzschia</i>	9.83%	No fold change
Medium centrics	6.43%	No fold change
Small centrics	6.28%	No fold change
Small <i>Pseudo-nitzschia</i>	3.24%	No fold change

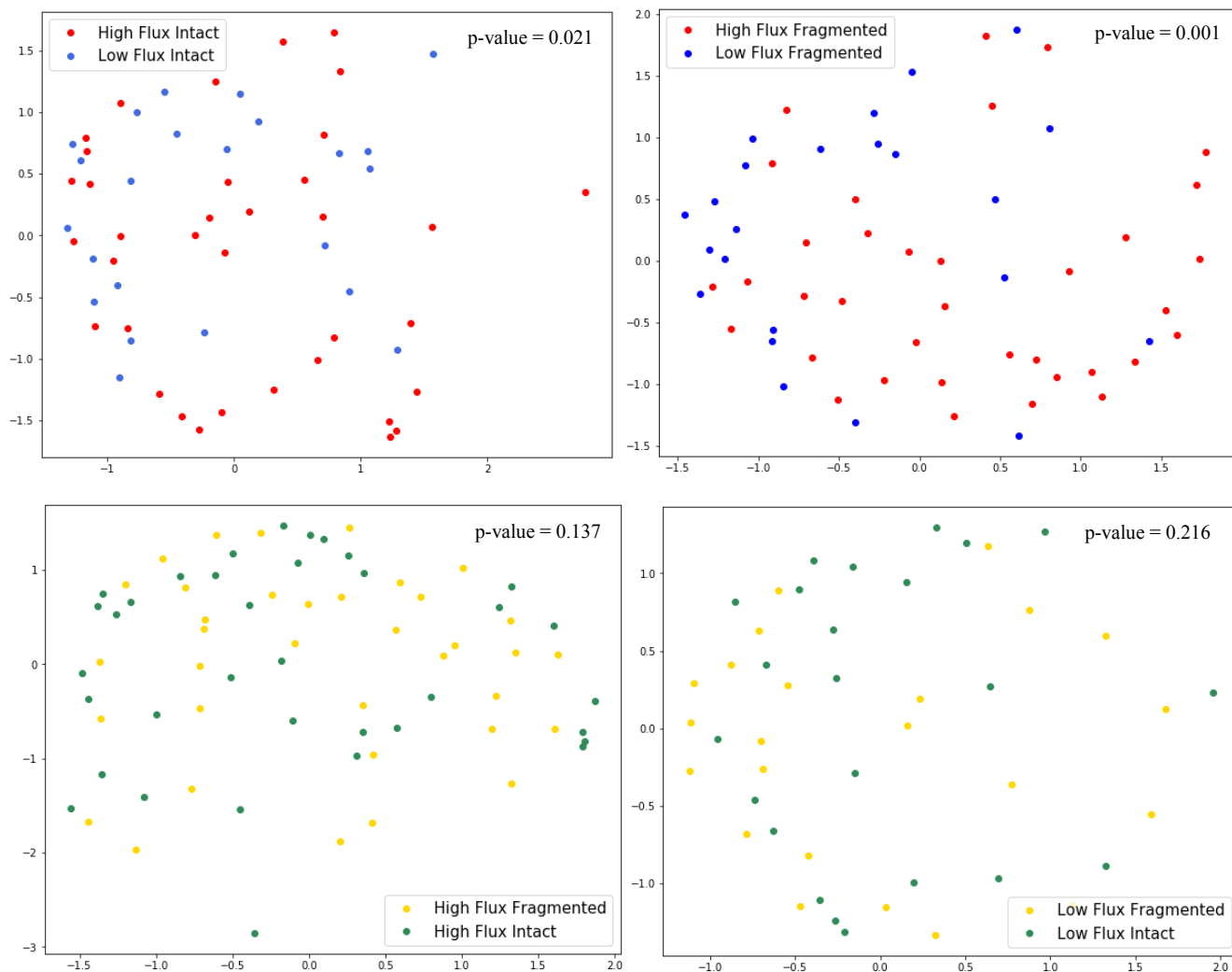


Figure 12. Top left: MDS plot of high-flux intact diatom and low-flux intact diatoms. No significant difference between the 2 groups (p-value = 0.021). Top right: MDS plot of high-flux fragmented diatoms, and low-flux fragmented diatoms. There are 2 distinct groups (p-value = 0.001). Bottom left: MDS plot of high-flux fragmented diatoms and high-flux intact diatoms. No significant difference between the 2 groups (p-value = 0.137). Bottom right: MDS plot of low-flux fragmented diatoms and low-flux intact diatoms. No significant difference between the 2 groups (p-value = 0.216).

We examined whether these data supported the ballast hypothesis by examining how biominerals, opal and CaCO_3 , changed as POC flux increased (Figure 13, top panels). The POC vs CaCO_3 and POC vs opal were positively linearly correlated. The slope of POC vs opal was 1.59 (p-value = 0.000002, standard error = 0.292) and the slope of POC vs CaCO_3 was 0.146 (p-value = 0.0051, standard error = 0.050). Although the correlations are statistically significant, they are relatively weak. The R-squared for POC vs opal was 0.375 and the R-squared for POC vs CaCO_3 was 0.142. The opal flux normalized to POC flux was not significantly linearly correlated to POC flux (slope = 0.18, p-value = 0.98, standard error = 9.44). The Mann-Whitney test comparing the median POC: opal fluxes during high-flux events versus low-flux periods indicate no significant enrichment or deficiency of opal during high-flux events (p=0.205). CaCO_3 flux normalized to POC flux was negatively linearly correlated with POC flux (slope = -3.23, p-value= 0.00032, standard error = 0.84) (Figure 13). The negative relationship indicates that higher POC samples contained lower amounts of CaCO_3 per unit POC. The Mann-Whitney test indicated significantly lower CaCO_3 : POC during the high-flux events (p=0.01). When three samples with the highest CaCO_3 :POC flux were removed from the analysis, there was no significant enrichment or deficiency of CaCO_3 during high-flux events (p= 0.019), suggesting that the reduced enrichment in CaCO_3 during high-flux events may not be a robust relationship.

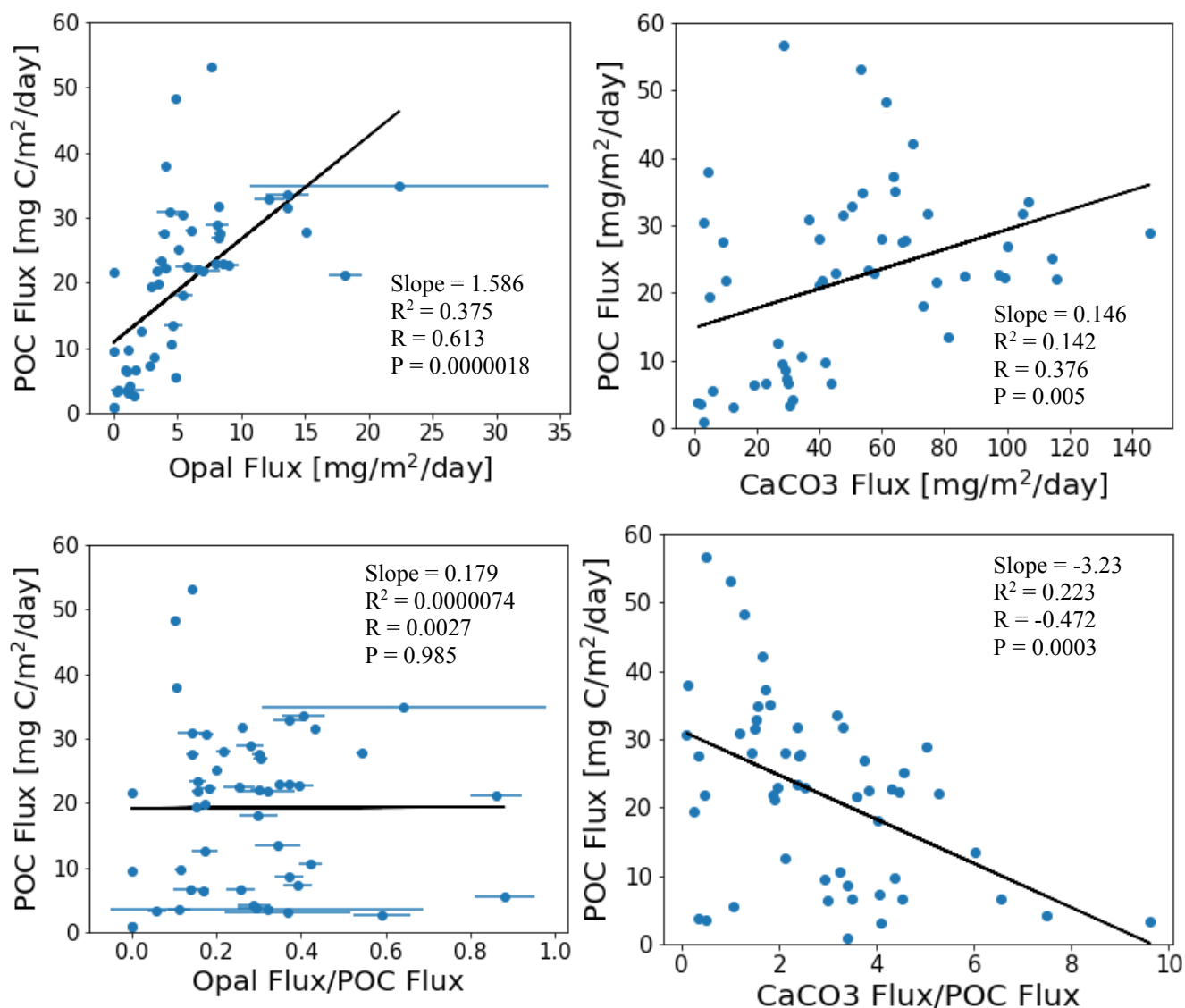


Figure 13. Regression analysis of Opal (top left) and CaCO₃ (top right) to test if there was a correlation between high-flux events and biomineral contents. Bottom left shows POC flux versus the ratio of Opal:POC and bottom right shows the POC flux versus the ratio of CaCO₃:POC.

DISCUSSION

Microscopic and chemical analysis of sinking particles enable us to identify ecological mechanisms involved in generating high-flux events at Station M. Our analysis suggests that particles contributing to high POC fluxes at Station M are first transformed and processed by deep ocean food webs on their journey to the bathypelagic. The original hypothesis stated that high-flux events are generated by rapid delivery of fresh phytodetritus that bypassed processing by deep ocean food webs. Although there was a greater absolute cell number flux in the samples collected during high-flux events compared to low-flux periods, cell number fluxes normalized to POC flux were lower during the high-flux events. There was a relatively constant POC: mass flux during the time series (Figure 5c), which indicates the freshness of material reaching the bathypelagic is unchanging. The normalized fragmented cell fluxes did not change, suggesting that the same relative amount of processed material was coming down, but relatively less fresh material during high-flux events (based on relatively less intact). The original hypothesis was that there was a large rapid increase of fresh, unprocessed particles sinking directly from the surface. However, fragmented phytoplankton cells showed that it was increased interactions and processing occurring in epipelagic and mesopelagic food webs.

The difference in community composition suggests that there are different types of cells and more processed cells sinking during the high-flux events compared to the low-flux periods. By understanding if the high-flux events' communities are made up of the same blooms as the low-flux periods' communities it would better indicate what types of mechanisms are causing the high-flux events. Intact-only communities were significantly different from each other with coccolithophores and diatoms influencing the differences in community composition. Fragmented diatoms were significantly different in high-and low-flux events, indicating changes in the fragmented diatoms were responsible for the difference in community composition as well (Figure 12 top right). This also suggests fragmented diatoms may be coming from different blooms at the surface rather than from the intact diatom cells. Analyzing closer we were able to infer

that both fragmented and intact diatom cells in high-flux events and in low-flux events were not significantly different from each other (Figure 12, bottom panels). This would suggest that intact and fragmented diatom cells during high-flux or low-flux events were coming from the same bloom communities in the surface. The fragmented diatom cells sinking during the high-flux events were significantly different from the fragmented diatom cells sinking during the low-flux event suggesting that the high-flux fragmented diatoms came from a different bloom than the low-flux fragmented diatom cells. Often, these blooms appear to have been dominated by the coastal genus *Skeletonema*, a known bloom-forming diatom. This would align with the introduction of different types of phytoplankton found in coastal versus offshore areas. The coastal communities mainly composed of diatoms would be transported offshore leading to a different community sinking. The fronts would carry the onshore blooms of diatoms offshore, allowing them to sink and contribute to the difference in community compositions for the fragmented diatoms. With differences in community composition, it is useful to understand the diversity within the samples. The diversity could indicate a bloom is dominated by a single type of phytoplankton cell. The Shannon diversity index indicated that there was no significant difference within the diversity of the high and low-flux events. There were no one type of phytoplankton dominating in either the high-flux events or low-flux periods.

Cell size was not a significant factor in causing high POC fluxes in the sediment trap, but the main difference was the fragmented versus intact cells. This was observed in the modeled carbon flux for diatoms. For intact diatoms the modeled relative carbon flux was significantly less during the high-flux events, but did not change for fragmented diatoms (Figure 8A, 10B). This indicates that the carbon flux associated with fragmented cells did not change between high-flux events and low-flux periods, but intact diatom cells transported relatively more carbon in low-flux periods and less during high-flux events. This result also stands for different size classes of the diatom cells. Large and small live diatoms transport relatively less carbon during high-flux events (Figure 11A), while large and small fragmented diatoms transport the same relative amount of carbon. Cell size was of interest due to their different physiological adaptations including forming large mats and migrating through the water column (Villareal, et al., 1996). If the cells

could migrate on their own and form large mats, then they could potentially increase the POC flux due to increased number of large cells. Phytoplankton cell size does not affect the POC flux, but fragmented cells are causing a significant change in POC flux during high-flux events. An important caveat in the modeled carbon data was that sometimes the total modeled carbon was greater than the total measured POC flux. The average modeled carbon flux by intact and fragmented diatoms was ~20% - 50% of the total measured carbon flux. This number is much higher than expected (Silver and Gowing, 1991). The average amount of carbon flux contained in phytoplankton cells has previously been estimated in mesopelagic sediment traps to be 3-20% (Silver and Gowing, 1991), and we would expect that contribution to decrease with increasing depth. The apparent overestimation of modeled diatom carbon flux is likely caused by fragmented cells being counted as separate cells, or intact cells' carbon content being attenuated as they sink to bathypelagic depths. Since the issue with fragmented cells' carbon content was addressed by looking at both fragmented and intact diatom cells separately, the likely cause would be the cells' carbon attenuation. The equation used to model the cells carbon was created on healthy live cultures and could be a reason carbon was so overestimated. Even though the modeled carbon was much higher than expected, it provided useful insight in the diversity of biovolumes among different species' carbon flux during high-flux events. The amount of carbon may be reduced as the cells sink causing the model calculations to give a much higher estimate. The overestimation of modeled carbon suggests that the cells are more processed as they sink to the bathypelagic.

The presence of chlorophyll within cells may indicate how quickly the cells were transported to the sediment traps. Particles sinking during the low-flux periods were more enriched in intact and chlorophyll-containing cells and could indicate that they were sinking quickly from the surface to the bathypelagic. Alternately, the enrichment of intact cells during low-flux periods could indicate that the epipelagic, mesopelagic and bathypelagic food webs were less efficient at intercepting sinking material and had overall lower grazing rates. This would lead to less processed and relatively more fresh cells sinking during low-flux periods.

It is not clear where exactly in the water column the processing is happening, but during high flux events particles could be encountering more grazing by zooplankton.

The zooplankton could be grazing in the mesopelagic as the phytoplankton cells sink or the zooplankton could graze the individual phytoplankton cells actively growing at the surface. There could also be more degradation by bacteria within the aggregates and fecal pellets, causing the cells within them to become highly processed and lose carbon. Bacterial degradation may not be a major cause because the particles are sinking relatively quickly (~10 days on average) (Smith et al., 2018) and not allowing time for the degradation to occur. As observed by Conte et al., (2001) the rapid supply of phytoplankton cells into the mesopelagic can stimulate the grazing response of deep-water ecosystems, and in turn deliver transformed particles to the bathypelagic. That indicates that higher magnitude of surface phytoplankton sinking through the water column can enhance more grazing in the mesopelagic the cells will encounter on their way down to the deep ocean.

A second hypothesis addressed in this study was that ballasting from biominerals within the phytoplankton aggregates cause high-flux events. We found a positive linear relationship between CaCO_3 and POC flux and a closer positive linear relationship between opal and POC flux (Figure 13, top panels). Much like the findings in Klaas and Archer (2002), there was an increase in both biominerals with increased POC. However, Klaas and Archer (2002) found a more statistically significant relationship between CaCO_3 and POC compared to the relationship between opal and POC. When comparing the R-value between the data in this study and Klaas & Archer (2002) the R-values for POC to opal fluxes are 0.613 and 0.328 respectively. The R-values for POC to CaCO_3 fluxes are 0.457 and 0.691, respectively. These data indicate that in this study the opal has a stronger correlation to POC than what was found by Klaas & Archer (2002), while the CaCO_3 does not have as strong of a correlation to POC. In contrast, the slope of CaCO_3 to POC flux was more similar to that found by Klaas and Archer (2002) than the slope of POC to opal flux. The slope of POC versus CaCO_3 measured was 0.146 which is very similar to the slope measured by Klaas and Archer (2002) (slope = 0.126). The slope of POC versus opal measured in this study was 1.59, which is steeper compared to the slope measured by Klaas and Archer (2002) study (slope = 0.061).

The steeper slope of POC versus opal flux indicates that there is less opal per unit POC in our dataset compared to previous studies. This result was unexpected because

diatoms make up most of the surface production in this coastal upwelling environment. These diatom blooms are fueled by relatively high concentrations of silicic acid in upwelled waters and with low silica dissolution in the surface water prior to sinking (Brzezinski et al., 2003). Additionally, iron limitation occurs in this region and causes surface diatom communities to become relatively more silicified (Hutchins & Bruland, 1998), enhancing export out of the surface (Brzezinski et al., 2015) and potentially transporting more opal as they sink to bathypelagic depths. Since the particles are generated from a diatom-rich iron-limited ecosystem with a high silicic acid concentration, then the expected result would be relatively more opal being transported during high-flux events. Instead, there is a much lower ratio of opal to POC fluxes in samples collected before, during, and after high-flux events. This could be due to either differences in our observational design compared to Klaas and Archer (2002) or enhanced dissolution of opal in the deep ocean at this location. We explore these two possibilities below.

Klaas and Archer (2002) analyzed sediment trap samples from different locations globally including open ocean samples. Our observations were collected from a single location off the coast of California in a very dynamic coastal system and was sampled over 29 years. Klaas and Archer (2002) were looking at many different locations over a minimum of a 10-month period over seasonal and geographic variations to see how the ballast hypothesis would apply to increasing POC at the different locations. The samples in this study included only those collected right before, during, and immediately after a high-flux event occurred to see if there were any indication as to what was causing the high-flux events and not represent the range of variation among seasons. If seasonal trends were added into this data set it would give us a whole picture of the opal flux at Station M including during the normal flux periods that do not respond to the high-flux events. In order to see a similar slope as Klaas and Archer (2002), the seasonal data would have to have a shallower slope suggesting more opal per unit POC. Although the information from year-round data would prove useful, it would not help tease apart the differences within high-flux events. The high-flux events still have less opal per unit POC with a much stronger correlation than POC versus CaCO_3 .

Dissolution and the loss of opal does occur in the water column as particles sink. This process would support the idea of highly processed particles sinking during the high-flux events. More dissolution could mean more mesopelagic grazing as the particles sink or degradation of particles from bacteria as they sink (Bidle et al., 2003). The cells that are sinking within the particles are sinking at a relatively fast rate approximately 10 days (Smith et al., 2018). This suggests that there is a short time where the cells can dissolve, and bacterial degradation may not play as big a role as zooplankton grazing. Most of the cells that could dissolve would already be dead or fragmented which we accounted for by separating intact versus fragmented cells in the analysis. In fact, the relative flux of cells most likely to dissolve (fragmented and empty frustules) did not change during high-flux events, unlike the intact cells. When cells are repackaged a coating of organic matter can slow the dissolution rates as the particles sink (Van Cappellen et al., 2002). We see less opal:POC suggesting that opal dissolved more before, during, and after the high-flux events, supporting the enhanced grazing of particles in the epipelagic/mesopelagic. This suggests that grazing allows for more dissolution in the water column. If dissolution played a role in the composition detected within the sediment traps, it did not mask our ability to detect changes between high- and low-flux periods. Since the samples were mostly composed of diatoms, which were easily identified and apparently preserved in the samples, and they were the primary driver of community changes during high-flux events, we can rule out dissolution as masking the influence of BSi on POC flux.

Particles sinking during high-flux events were not enriched in biominerals, suggesting that ballasting was not responsible for high-flux events in the bathypelagic. There was a negative relationship between POC vs. CaCO_3 : POC (Figure 13, bottom right), indicating that there was relatively more CaCO_3 sinking during the low-flux periods and relatively less CaCO_3 flux during the high-flux events. But, when the three samples with the highest CaCO_3 fluxes were removed from the data, there was no difference in CaCO_3 : POC during high-flux events compared to low-flux periods. This finding suggests that the apparent reduction in relative CaCO_3 fluxes in high-flux events is only weakly supported. However, these data are consistent with the reduction in relative coccolithophore number fluxes in particles during the high-flux events. In

contrast, the POC vs opal flux did not change during high-flux events (Figure 13, bottom left), which is consistent with the sustained influence of fragmented diatom frustules in spite of the relative reduction of intact diatom cell fluxes during the high-flux events. Interestingly, the highest opal measurements occurred during moderate POC fluxes and not during the highest POC flux events. This suggests that biomineral ballasting may not be responsible for increasing the amount of POC flux during high-flux events, but instead indicates change in ecological interactions responsible for driving increasing POC fluxes.

Another alternative way to assess biomineral fluxes is in the context of POC flux transporting biominerals. According to Passow & De La Rocha, (2006), the POC flux determines the flux of minerals to the deep ocean, and not vice versa. They found that smaller aggregates contained more minerals and that aggregates were good at picking up suspended minerals in the water column. The POC: mineral ratio is a function of how much suspended mineral is accumulated as the aggregates sink, and therefore the minerals do not ballast the aggregates. Lampitt et al., (2009) measured particulate organic matter in the north east Atlantic at station PAP. They showed ~ 60% of the POC flux occurred when mineral flux was at its lowest which is contradictory to the ballast hypothesis idea (Lampitt et al., 2009). This suggests that the ballasting may not be the cause of higher POC flux, but instead that POC may be driving the mineral flux. Lampitt et al. (2009) found that the percent of BSi to POC was constant with increased POC flux. This result relates to the data found in this study where the normalized BSi was constant with increased POC flux.

The data show that fragmented cells are driving the high-flux events suggesting that grazing in the epipelagic and mesopelagic was enhanced during the high-flux events, but there should be some consideration in the limitations of the data. The first limitation to address is the counting uncertainty. A small subsample of each sample was taken and then diluted by 10-15 times to allow for no overcrowding. Cells still embedded within particularly sturdy aggregates and fecal pellets would not have been counted due to not being picked up by the 1mL pipettor. A large portion of cells could have broken out of these large particles when collected from the trap, when mixed in the lab, and when the samples went through multiple freezing and thawing periods. Although we did make sure to account for 80% of the total species that could have been observed in the samples,

there still might have been some rare cells that were missed or some larger cells that were not detected. We are confident in the assessment of the community composition and even though some rare cells were not accounted for, this would not have an important impact on the results. Other limitations that could be affecting the data include that some samples were missing from the archive of samples. This could affect some of the outcomes, although there were only 7 missing samples out of 70 total samples.

To account for some variations within the biogenic silica analysis triplicate subsamples were measured. The three 200 μ L subsamples were measured to account for variation in particles within the small volume measured. There was little variation (average \sim 16%) among the triplicates indicating that the subsample accurately represented the total sample. PIC data was not available for all the samples meeting the criteria for the experimental design. There were 10 samples missing from the total 65 samples. Even though some samples were missing, the samples analyzed depicted overall trends and major changes.

Along with the limitations of the BSi data, some cells containing BSi likely dissolved as they sank through the water column. When dead cells sink, their silica can dissolve which could affect the amount of BSi detected in the sediment traps. Within a trap cup, the dissolution of BSi does not seem to be above 10% of total BSi in particles annually collected in traps (Klaas & Archer, 2002). This could be because the high dissolution rates tend to occur more during low-flux periods. Understanding the amount of dissolution taking place in the water column can help us understand the different mechanisms occurring for cells containing BSi. There are also studies that look at different preservatives that can affect the dissolution within the traps. In formalin preserved traps it was found that $5\pm 2\%$ of the BSi within cells will be soluble in the preserved trap (Honjo et al., 1995). Knowing that formalin can affect the dissolution as well that is something that could be addressed in future studies, but since the percentage is so low the data in this study will not change drastically even if the dissolution is accounted for in the traps.

Identifying which mechanisms are most influential in generating high-flux events can help focus new observational efforts intended to better resolve the processes driving changing POC flux in the California Current. While it is difficult to directly identify

mechanisms causing high-flux events, our observations indicate that midwater ecosystems play a large role in generating the high-flux events that eventually reach the bathypelagic at Station M. These ecosystems are fueled by large, rapid influxes of sinking surface material, increasing grazing by the epipelagic and mesopelagic zooplankton. Ballasting also does not seem to be the cause of increased POC from the mesopelagic to bathypelagic depths. Direct export of fresh, large-celled diatom blooms also does not appear to be driving these high-flux events. With these results in mind, we suggest focusing observational efforts on quantifying the fecal pellets and aggregates sinking along with the phytoplankton and zooplankton to better quantify where the majority of carbon is coming from and if the fecal pellets are playing a large role in the carbon flux to the deep ocean. Understanding how the cells are packaged (fecal pellet or aggregates) when they are captured in the trap will help us determine the ecological mechanism transporting cells. If we see more cells packaged in fecal pellets, we could hypothesize that there was a lot of zooplankton grazing in the epipelagic and mesopelagic and repackaging of POC into rapidly sinking pellets. If aggregates are more common during high-flux events, then cells are sticking together, which may indicate lower nutrients at the surface or more processing and degradation. One way to make these observations is with the SES (sedimentation event sensor), a time-lapse in situ imaging sediment traps (Huffard et al., 2020). The SES can quantify the relative fluxes of aggregates and various fecal pellets types every 2 hours. This would help answer the question of what type of particle is sinking during the high-flux event. During an 8-month time period, Huffard et al. (2020) at Station M found that salp fecal pellets delivered ~45% of the total POC flux and aggregates were of lower quality particles probably due to lateral advection. If the aggregates were of lower quality, it could suggest that more processes including enhanced grazing in the epipelagic and mesopelagic were occurring before the particles reached the bathypelagic. Using this in-situ imaging information alongside microscopy, we could better understand the processes the phytoplankton cells are going through before being collected in the sediment traps.

DNA metabarcoding of the community within sinking particles in combination with microscope counts would better resolve the entire community within sinking particles during the high-flux events and low-flux periods. The genetic data would detect

if a new species was present during the high-flux events that was not observed before, whereas microscopy would give a more quantitative depiction of the cell types collected. Preston et al. (2020) used DNA metabarcoding of particles at Station M to determine how community composition within particles changed over time. They found that diatoms that likely originated from coastal blooms dominated a seasonal high POC flux event and suggested that zooplankton grazing on diatom communities led to a rapid transport of POC. Preston et al. (2020) identified *Thalassiosira* as a key cell type found in high-flux events. In this study, fragmented centric diatoms, likely *Thalassiosira*, were important for the historically high-flux events. By sequencing genetic markers, we would be able to capture cells not easily distinguished by microscopy. This would help answer the question of which types of phytoplankton are more dominant in high-flux events.

Another way to understand the mechanisms of the sinking phytoplankton cells would be to access satellite data off the coast of California at the time of different events. Some data has been collected to show time lags (0-70 days) between surface chlorophyll data and satellite-estimated export flux and POC flux to deep ocean (Smith et al. 2018). They found variability between surface ocean conditions and the transport of organic carbon to the deep ocean. The time lags with surface chlorophyll and POC transport can be used to see how different events of phytoplankton blooms can affect the delivery of carbon to the deep ocean. Another forcing mechanism not measured in this study is the physical dynamics that are taking place in the California Current System which affect the export of cells. This highly dynamic environment causes nutrient upwelling, allowing the phytoplankton blooms to form. Stukel et al. (2017) showed that submesoscale and mesoscale fronts along the California Current System are a place of high primary production which can lead to high export of carbon in those areas. These high carbon export events have been observed, due to physical subduction and a sinking hotspot. Diatoms can make up 25% of the primary production at the fronts (Krause et al., 2015). The diatoms have a large impact on the surface primary production in the fronts and if they ultimately sink will transport carbon or serve as a ballast for carbon in fecal pellets. Larger aggregates have been observed along with increased diatoms at frontal regions (Yoder et al., 1994). The observations in this study have shown that enhanced epipelagic and mesopelagic food webs have a great impact on the POC fluxes. This leads to a new

hypothesis suggesting increases of POC export in the California Current System allows the enhanced epipelagic and mesopelagic food web processes to occur at frontal systems in this region which in turn transports large aggregates of highly processed diatom cells to the bathypelagic.

A more comprehensive analysis of the sediment trap samples would also better resolve what is distinct about high-flux samples. If the community composition with low-flux samples over the entire time-series and across seasons were compared to the low-flux periods occurring before or after the high-flux events, it would better distinguish the most important features of the high-flux events. There is also a seasonality pattern seen where the high-flux events occur in the spring through fall period, so there must be a different process happening in the winter, likely lack of primary production at the surface or lack of upwelling, that prevents high-flux events from occurring during that season. Comparing the whole time series will help fill in the gaps with seasonality and different processes occurring at different time periods.

CONCLUSIONS

- Distinct community composition of phytoplankton cells contributing to high-flux events
- Fragmented cells are contributing to both high-flux events and low-flux periods at the same rate meaning that zooplankton grazing may be generating the high-flux events
- Intact cells, containing chlorophyll, were relatively less enriched in particles and transported relatively less of the carbon to the deep ocean during high-flux events.
- High POC flux events did not appear to be influenced by cells of a particular size class.
- Opal fluxes were relatively the same during high-flux events, while CaCO_3 fluxes were relatively low during high POC fluxes
- Ballasting does not appear to be responsible for higher POC fluxes occurring at Station M. More likely, the high POC fluxes actually are the mechanism driving increases in the mineral fluxes.

- The mechanism controlling high-flux events are most likely processes occurring in the epipelagic and mesopelagic. Rapid sinking (~10 days) of diatom blooms from the surface waters likely enhances mesopelagic food webs and generates rapidly sinking, processed particles. This could explain the relative dominance of fragmented cells within sinking particles that reach bathypelagic depths during high-flux events at Station M.

REFERENCES

- Armstrong, R. A., Lee, C., Hedges, J. I., Honjo, S., & Wakeham, S. G. (2002). A new, mechanistic model for organic carbon fluxes in the ocean based on the quantitative association of POC with ballast minerals. *Deep-Sea Research Part II: Topical Studies in Oceanography*, 49(1–3), 219–236. [https://doi.org/10.1016/S0967-0645\(01\)00101-1](https://doi.org/10.1016/S0967-0645(01)00101-1)
- Bakun, A., Black, B. A., Bograd, S. J., García-Reyes, M., Miller, A. J., Rykaczewski, R. R., & Sydeman, W. J. (2015). Anticipated Effects of Climate Change on Coastal Upwelling Ecosystems. *Current Climate Change Reports*, 1(2), 85–93. <https://doi.org/10.1007/s40641-015-0008-4>
- Bidle, K. D., Brzezinski, M. A., Barbara, S., Long, R. A., & Jones, J. L. (2003). Diminished efficiency in the oceanic silica pump caused by bacteria-mediated silica dissolution. *Limnology and Oceanography*, 48(5), 1855–1868.
- Brzezinski, M. A., Jones, J. L., Barbara, S., Bidle, K. D., & Azam, F. (2003). The balance between silica production and silica dissolution in the sea : Insights from Monterey Bay , California , applied to the global data set. *Limnology and Oceanography*, 48(5), 1846–1854.
- Brzezinski, M. A., Krause, J. W., Bundy, R. M., Barbeau, K. A., Franks, P., Goericke, R., ... & Stukel, M. R. (2015). Enhanced silica ballasting from iron stress sustains carbon export in a frontal zone within the California Current. *Journal of Geophysical Research: Oceans*, 120(7), 4654–4669.
- Chao, A., Colwell, R. K., Lin, C. W., & Gotelli, N. J. (2009). Sufficient sampling for asymptotic minimum species richness estimators. *Ecology*, 90(4), 1125–1133. <https://doi.org/10.1890/07-2147.1>
- Conte, M. H., Ralph, N., & Ross, E. H. (2001). Seasonal and interannual variability in deep ocean particle fluxes at the Oceanic Flux Program (OFP)/Bermuda Atlantic Time Series (BATS) site in the western Sargasso Sea near Bermuda. *Deep-Sea Research Part II: Topical Studies in Oceanography*, 48(8–9), 1471–1505. [https://doi.org/10.1016/S0967-0645\(00\)00150-8](https://doi.org/10.1016/S0967-0645(00)00150-8)

- Ducklow, H. H. W., Steinberg, D. D. K., Buessler, K., & Buesseler, K. O. (2001). Upper ocean carbon export and the biological pump. *Oceanography*, *14*(4), 50–58. <https://doi.org/10.5670/oceanog.2001.06>
- Honjo, S., Dymond, J., Collier, R., & Manganini, S. J. (1995). Export production of particles to the interior of the equatorial Pacific Ocean during the 1992 EqPac experiment. *Deep-Sea Research Part II*, *42*(2), 831–870.
- Huffard, C. L., Durkin, C. A., Wilson, S. E., McGill, P. R., Henthorn, R., & Smith, K. L. (2020). Temporally-resolved mechanisms of deep-ocean particle flux and impact on the seafloor carbon cycle in the northeast Pacific. *Deep-Sea Research Part II: Topical Studies in Oceanography*, *xxxx*, 104763. <https://doi.org/10.1016/j.dsr2.2020.104763>
- Hutchins, D. A., Bruland, K. W., & Cruz, S. (1998). Iron-limited diatom growth and Si:N uptake ratios in a coastal upwelling regime. *Nature*, *393*(6685), 561-564. <https://doi.org/10.1038/31203>
- Kahru, M., Kudela, R. M., Manzano-sarabia, M., & Mitchell, B. G. (2012). Deep-Sea Research II Trends in the surface chlorophyll of the California Current : Merging data from multiple ocean color satellites. *Deep-Sea Research Part II*, 1–10. <https://doi.org/10.1016/j.dsr2.2012.04.007>
- Karl, D. M., Church, M. J., Dore, J. E., Letelier, R. M., & Mahaffey, C. (2012). Predictable and efficient carbon sequestration in the North Pacific Ocean supported by symbiotic nitrogen fixation. *Proceedings of the National Academy of Sciences of the United States of America*, *109*(6), 1842–1849. <https://doi.org/10.1073/pnas.1120312109>
- Kemp, A. E. S., Pike, J., Pearce, R. B., & Lange, C. B. (2000). The “Fall dump” - A new perspective on the role of a “shade flora” in the annual cycle of diatom production and export flux. *Deep-Sea Research Part II: Topical Studies in Oceanography*, *47*(9–11), 2129–2154. [https://doi.org/10.1016/S0967-0645\(00\)00019-9](https://doi.org/10.1016/S0967-0645(00)00019-9)
- Klaas, C., & Archer, D. E. (2002). Association of sinking organic matter with various types of mineral ballast in the deep sea: Implications for the rain ratio. *Global Biogeochemical Cycles*, *16*(4), 63-1-63–14. <https://doi.org/10.1029/2001GB001765r>
- Krause, J. W., Brzezinski, M. A., Goericke, R., Landry, M. R., Ohman, M. D., Stukel, M.

- R., & Taylor, A. G. (2015). Variability in diatom contributions to biomass, organic matter production and export across a frontal gradient in the California Current Ecosystem. *Journal of Geophysical Research: Oceans*, *120*(2), 1032-1047.
- Lamborg, C. H., Buesseler, K.O., Valdes, J., Bertrand, CH., Bidigare, R., Manganini, S., ... & Wilson, S. (2008). The flux of bio-and lithogenic material associated with sinking particles in the mesopelagic “twilight zone” of the northwest and North Central Pacific Ocean. *Deep Sea Research Part II: Topical Studies in Oceanography*, *55*(14-15), 1540-1563.
- Lampitt, R. S., Salter, I., & Johns, D. (2009). Radiolaria: Major exporters of organic carbon to the deep ocean. *Global Biogeochemical Cycles*, *23*(1), 1–9.
<https://doi.org/10.1029/2008GB003221>
- Le Moigne, F. A. C., Pabortsava, K., Marcinko, C. L. J., Martin, P., & Sanders, R. J. (2014). Where is mineral ballast important for surface export of particulate organic carbon in the ocean?. *Geophysical Research Letters*, *41*(23), 8460–8468.
<https://doi.org/10.1002/2014GL061678>
- Menden-Deuer, S., & Lessard, E. J. (2000). Carbon to volume relationship for dinoflagellates, diatoms and other protist plankton. *Limnology and Oceanography*, *45*(3), 569–579.
<https://aslopubs.onlinelibrary.wiley.com/doi/pdf/10.4319/lo.2000.45.3.0569>
- Passow, U., & De La Rocha, C. L. (2006). Accumulation of mineral ballast on organic aggregates. *Global Biogeochemical Cycles*, *20*(1), 1–7.
<https://doi.org/10.1029/2005GB002579>
- Preston, C. M., Durkin, C. A., & Yamahara, K. M. (2020). DNA metabarcoding reveals organisms contributing to particulate matter flux to abyssal depths in the North East Pacific ocean. *Deep-Sea Research Part II: Topical Studies in Oceanography*, *August*, 104708. <https://doi.org/10.1016/j.dsr2.2019.104708>
- Ragueneau, O., Leynaert, A., Tréguer, P., Demaster, D. J., & Anderson, R. F. (1996). Opal studied as a marker of paleoproductivity. *Eos, Transactions American Geophysical Union*, *77*(49), 491–491. <https://doi.org/10.1029/96EO00325>
- Silver, M. W., & Gowing, M. M. (1991). The “particle” flux: origins and biological components. *Progress in Oceanography*, *26*(1), 75-113.

- Smith, K. L., & Druffel, E. R. M. (1998). Long time-series monitoring of an abyssal site in the NE Pacific: An introduction. *Deep-Sea Research Part II: Topical Studies in Oceanography*, 45(4–5), 573–586. [https://doi.org/10.1016/S0967-0645\(97\)00094-5](https://doi.org/10.1016/S0967-0645(97)00094-5)
- Smith, Kenneth L., Ruhl, H. A., Huffard, C. L., Messié, M., & Kahru, M. (2018). Episodic organic carbon fluxes from surface ocean to abyssal depths during long-term monitoring in NE Pacific. *Proceedings of the National Academy of Sciences*, 201814559. <https://doi.org/10.1073/pnas.1814559115>
- Smith, Kenneth L, Ruhl, H. a, Kahru, M., Huffard, C. L., & Sherman, A. D. (2013). Deep ocean communities impacted by changing climate over 24y in the abyssal northeast Pacific Ocean. *Proceedings of the National Academy of Sciences*, 110(49), 19838–19841. <https://doi.org/10.1073/pnas.1315447110/-/DCSupplemental.www.pnas.org/cgi/doi/10.1073/pnas.1315447110>
- Strickland, J. D. H., & Parsons, T. R. (1972). A practical handbook of seawater analysis.
- Stukel, M. R., Aluwihare, L. I., Barbeau, K. A., Chekalyuk, A. M., & Goericke, R. (2017). Mesoscale ocean fronts enhance carbon export due to gravitational sinking and subduction. *Proceedings of the National Academy of Sciences*, 114(6), 1252–1257. <https://doi.org/10.1073/pnas.1609435114>
- Thiel, H. Pfannkuche, O., Schriever, G., Lochte, K., Gooday, A. J., Hemleben, C., ... & Riemann, F (1988). Phytodetritus on the deep-sea floor in a central oceanic region of the northeast Atlantic. *Biological Oceanography*, 6(2), 203–239. <https://doi.org/10.1080/01965581.1988.10749527>
- Van Cappellen, P., Dixit, S., & van Beusekom, J. (2002). Biogenic silica dissolution in the oceans: Reconciling experimental and field-based dissolution rates. *Global Biogeochemical Cycles*, 16(4), 23-1-23–10. <https://doi.org/10.1029/2001gb001431>
- Venrick, E. L., Division, I. O., Diego, S., & Jolla, L. (2015). Phytoplankton Species in the California Current System off Southern California: the Spatial Dimensions. California Cooperative Oceanic Fisheries Investigations Reports, 56(2012), 168–184.
- Villareal, T. A., Woods, S., Moore, J. K., & Culver-, K. (1996). Vertical migration of Rhizosolenia mats and their significance to NO₃ fluxes in the central North Pacific gyre. *Journal of Plankton Research*, 18(7), 1103–1121.
- Volk, T., & Hoffert, M. I. (1985). Ocean carbon pumps: Analysis of relative strengths

and efficiencies in ocean-driven atmospheric CO₂ changes. *The carbon cycle and atmospheric CO₂: natural variations Archean to present*, 32, 99-110.

Yoder, J. A., Ackleson, S.G., Barber, R.T., Flament, P., & Balch, W.M. (1994). Aline in the sea. *Nature*, 371(6499), 689-692.

APPENDIX A
SUPPLEMENTARY INFORMATION

Table 1: Table of cell types counted and their corresponding carbon per cell (pgC/cell).

Cell Type	Carbon per cell (pgC/cell)
<i>Actinoptychus</i>	325.2919033
<i>Asteromphalus sarcophagus</i>	90.88024297
<i>Bacteriastrum</i>	105.4411389
<i>Ceratulina</i>	15.6873516
<i>Chaetoceros</i>	308.304
Centric Large	20615.87992
Centric medium	513.3032004
Centric small	126.0358502
<i>Delphineis</i>	36.94643651
<i>Ditylum</i>	1890.571444
<i>Eucampia</i>	147.5414802
<i>Fragilariopsis doliolus</i>	50.95966343
<i>Guinardia</i>	400.0571514
<i>Rhizosolenia</i> large	25924.86172
<i>Rhizosolenia</i> medium	6814.009344
<i>Rhizosolenia</i> small	1013.034303
<i>Skeletonema</i>	16.87653272
<i>Thalassiosira aestivalis</i>	247.2628236
<i>Thalassiosira rotula</i>	1534.596789
<i>Thalassionema</i>	14.3775026
<i>Nitzschia bicapitata</i>	12.08039021
<i>Nitzschia</i> medium	39.7350698
<i>Nitzschia</i> small	27.73842599
<i>Nitzschia sicula</i>	48.11660294
<i>Pleurosigma</i>	133.0677133

<i>Pseudo-nitzschia</i> large	104.5783796
<i>Pseudo nitzschia</i> small	64.39834045
<i>Manguinea fusiformis</i>	277.792756
<i>Proboscia</i>	114.7629589
<i>Coccolithus</i>	338.4691984
<i>Gephyrocapsa</i>	19.64176647
<i>Emeliana</i>	19.64176647
<i>helicosphaera</i>	216.2446953
<i>dictyocha</i>	668.1258463
rhizaria	11524.23
dinoflagellates	460.5744
Nanoflagellates	23.86265046
Silicic dinoflagellates	179.0071611
protists	535.89717
ciliates	11919.57

Table 2: Table of all samples with corresponding data (POC flux, PIC flux, BSi flux, carbon per cell flux, and cell number flux)

Sample Name	Date Open	Date Closed	Event Number	Event Period	POC Flux (mg/m ² /day)	PIC Flux (mg/m ² /day)	BSi Flux (mg/m ² /day)	Cellular POC Flux (mg/m ² /day)	Cell Number Flux (cells/m ² /day)
4211_1	10/14/2003	10/24/2003	1	Before	6.388895149	2.285206	0.070120	4.957298	33440000
4211_3	11/3/2003	11/13/2003	1	During	27.58247943	7.971191	0.125161	15.698297	114670400
4211_4	11/13/2003	11/23/2003	1	During	23.45031433	6.670402	0.065189	9.117859	60745600
4211_9	1/2/2004	1/12/2004	1	After	0.879265975	0.359315	0	0.921316	8467200
4302_11	6/7/2004	6/17/2004	2	Before	3.186901159	3.67213	0.024879	2.293786	8126976
4407_1	8/2/2004	8/12/2004	2	During	22.42418163	10.34494	0.106128	3.549717	37632000
4407_4	9/1/2004	9/11/2004	2	After	6.662726432	5.22384	0.058288	2.879994	17027258.18
5105_7	4/4/2007	4/14/2007	3	Before	13.523117	9.749633	0.143797	5.000686	21447876.92
5105_11	5/14/2007	5/24/2007	3	During	22.25426263	11.91564	0.075668	4.332626	17849454.55
5203_1	6/8/2007	6/18/2007	3/4	After/Before	9.55278304	3.370641	0	0.467947	3114947.368
5203_2	6/18/2007	6/28/2007	4	During	21.54900096	9.297585	0	0.377462	4410978.462
5203_3	6/28/2007	7/8/2007	4	During	31.68908889	12.56858	0.108002	11.756058	22238400
5203_4	7/8/2007	7/18/2007	4	During	22.69456601	11.69422	0.164359	8.061267	20094171.43
5203_5	7/18/2007	7/28/2007	4	During	18.1398624	8.745898	0.124288	5.089680	21357056
5203_6	7/28/2007	8/7/2007	4	During	28.96775727	17.46464	0.116603	6.561535	28731428.57
5203_7	8/7/2007	8/17/2007	4	During	21.97843586	13.89172	0.124984	5.197103	22490584.62
5203_8	8/17/2007	8/27/2007	4	During	25.18757043	13.72113	0.083718	4.207274	20950080
5203_11	9/16/2007	9/26/2007	4	After	9.59136621	4.51025	0.047823	4.687138	10572231.11
5704_19	5/8/2011	5/18/2011	5	Before	4.224736331	3.792676	0.120288	4.760743	17033142.86
5805_3	6/15/2011	6/25/2011	5	During	53.13500147	6.387725	0.059867	22.308190	33862400
5805_4	6/25/2011	7/5/2011	5	During	31.52315954	5.694519	5.693292	38.735714	35472640
5805_5	7/5/2011	7/15/2011	5	During	34.82920046	6.458226	0.267564	42.533180	78323200
5805_6	7/15/2011	7/25/2011	5	During	21.08293678	4.765486	0.358700	35.375821	69005440
5805_7	7/25/2011	8/4/2011	5	During	27.74077346	8.114162	0.225798	34.596200	45168853.33
5805_8	8/4/2011	8/14/2011	5	During	22.97239805	5.428111	0.154943	21.171928	76869333.33
5805_9	8/14/2011	8/24/2011	5	During	22.94051952	6.917954	0.144614	8.971072	59875200
5805_10	8/24/2011	9/3/2011	5/6	After/Before	10.56027902	4.091766	0.176162	24.970919	38966400
5805_18	11/12/2011	11/18/2011	6	During	26.89485604	12.46307	0.126666	21.592399	47232814.97
5908_2	12/1/2011	12/11/2011	6	After	3.742545579	1.414416	0.122387	5.147175436	21050040
5908_8	8/4/2011	8/14/2011	7	Before	3.487362692	2.223465	0.046753	3.539836	16264045.71
5908_12	3/10/2012	3/20/2012	7	During	21.78178967	12.85247	0.064456	19.1225493	49884800
5908_13	3/20/2012	3/30/2012	7	During	27.50105164	11.75	0.059629	31.17917447	137193600
5908_14	3/30/2012	4/9/2012	7	During	19.29514624	6.442651	0.063327	11.51845358	27224000
5908_15	4/9/2012	4/19/2012	7	During	37.99381189	6.678305	1.669399582	12.3165093	10028683.6
5908_18	5/9/2012	5/19/2012	7	During	30.54794633	4.514366	0.073226	13.496943	114105600
5908_21	6/8/2012	6/12/2012	7	After	2.591358	ND	0.637694647	11.517017	32929929.39
6005_2	6/24/2012	7/4/2012	8	Before	0.92438	ND	0.000545774	1.478679	13761600
6107_2	11/28/2012	12/8/2012	8	After	3.050586	1.490807	0.469357772	1.593255345	9705658.182
6107_21	6/6/2013	6/15/2013	9	Before	5.514221	0.664627	2.022213882	1.605148	8061840.9
6607_8	3/8/2016	3/25/2016	10	Before	3.485129419	ND	0.133163	12.413640	19690666.67
6607_10	4/11/2016	4/28/2016	10	During	33.54482067	12.83747	0.168876	71.774075	48684100.84
6607_11	4/28/2016	5/15/2016	10	After	7.268820847	3.535718	0.163209	8.167814	25005176.47
6607_13	6/1/2016	6/18/2016	11	Before	8.586689839	3.493678	0.154556	16.184459	19670588.24

6607_14	6/18/2016	7/5/2016	11	During	56.73218541	3.407647	ND	235.450906	121054870.6
6607_16	7/22/2016	8/8/2016	11	After	6.546783675	2.738176	0.69884	30.146929	21184289.59
6607_19	9/11/2016	9/28/2016	12	During	19.92714616	ND	0.072449	23.438711	47487472.94
6607_20	9/28/2016	10/15/2016	12	During	28.12069327	7.154864	ND	38.782889	75728414.12
6607_21	10/15/2016	11/1/2016	12	During	32.91835462	6.067914	0.154235	31.665891	37010823.53
6805_1	7/4/2017	7/15/2017	13	During	6.6	3.622521	ND	6.862213	16440103.9
6805_9	6/23/2017	7/4/2017	13	During	47.2	ND	ND	30.182717	46385870.13
6805_10	7/4/2017	7/15/2017	13	During	37.3	7.63971	ND	82.002729	69063272.73
6805_11	7/15/2017	7/26/2017	13	During	31.7	8.960678	ND	40.120520	40800000
6805_15	8/28/2017	9/8/2017	13	During	35.1	7.665316	ND	24.258891	26378181.82
6805_16	9/8/2017	9/19/2017	13	During	42.1	8.360975	ND	21.124731	32491636.36
6805_17	9/19/2017	9/30/2017	13	During	28.1	4.809215	0.090335	15.307647	41981922.08
6805_18	9/30/2017	10/11/2017	13	During	21.8	4.893319	0.133614	11.46400109	39427200
6805_19	10/11/2017	10/22/2017	13	During	30.8	4.375013	0.060047	8.652781	9847854.545
6805_20	10/22/2017	11/2/2017	13/14	After/Before	12.6	3.191936	0.072536	8.074386	16376727.27
6805_21	11/2/2017	11/13/2017	14	During	48.3	7.354254	2.033882183	19.203293	41339810.91

Table 3: Tables of all samples for BSi analysis including absorbance and standard deviation of the mean absorbance.

Sample Name	POC (mgC m ⁻² day ⁻¹)	Date Open	Date Closed	dilution	filter blank	slope	sample filtered (L)	blank	absorbance	sample volume (mL)	Silica flux [mg/m ² /day]	BSi Standard Deviation
58_4	31.52316	6/25/2011	7/5/2011	10	0.018939	0.17755	0.0001	0.055	0.84	22.2	5.693292	0.070019713
66_16A	6.546784	7/22/2016	8/8/2016	1	0.018939	0.17755	0.0001	0.055	0.763333	76.2	0.698844	0.090891572
58_3	53.135	6/15/2011	6/25/2011	10	0.018939	0.17755	0.0001	0.055	0.996667	10.4	3.181026	0.115196935
58_8	22.9724	8/4/2011	8/14/2011	10	0.018939	0.17755	0.0001	0.055	0.513333	23.2	3.559404	0.256977778
58_10	10.56028	8/24/2011	9/3/2011	10	0.018939	0.17755	0.0001	0.055	0.266667	24.6	1.860324	0.118519784
58_7	27.74077	7/25/2011	8/4/2011	10	0.018939	0.17755	0.0001	0.055	0.693333	29.8	6.263821	0.143572746
59_13	27.50105	3/20/2012	3/30/2012	10	0.018939	0.17755	0.0001	0.055	0.166667	37.2	1.639869	0.179225039
66_8B	3.485129	3/8/2016	3/25/2016	1	0.018939	0.145983	0.0001	0.038333	0.38	92.3	0.464092	0.533963415
58_5	34.8292	7/5/2011	7/15/2011	13.33333333	0.018939	0.145983	0.0001	0.038333	0.846667	21.1	9.319049	4.869520413
59_15	37.99381	4/9/2012	4/19/2012	10	0.018939	0.1654	0.0001	0.045	0.253333	21.6	1.6694	0.111710672
59_14	19.29515	3/30/2012	4/9/2012	10	0.018939	0.1654	0.0001	0.045	0.17	24.9	1.221907	0.146020051
58_9	22.94052	8/14/2011	8/24/2011	10	0.018939	0.1654	0.0001	0.045	0.433333	24	3.317524	0.046914073
59_12	21.78179	3/10/2012	3/20/2012	10	0.018939	0.1654	0.0001	0.045	0.183333	26.2	1.403977	0.102429059
59_8	3.487363	1/30/2012	2/9/2012	1	0.018939	0.1654	0.0001	0.045	0.486667	20.4	0.163045	0.038040197
58_18	26.89486	11/12/2011	11/18/2011	10	0.018939	0.1654	0.0001	0.045	0.283333	24.2	3.406661	0.201483189
59_2	3.742546	12/1/2011	12/11/2011	1	0.018939	0.1654	0.0001	0.045	0.86	22.2	0.45804	0.065093276
66_11B	7.268821	4/28/2016	5/15/2016	10	0.018939	0.1654	0.0001	0.045	0.206667	32.8	1.186336	0.099785132
58_6	21.08294	7/15/2011	7/25/2011	10	0.018939	0.1654	0.0001	0.045	0.79	29.2	7.562448	0.523135737
66_13A	8.58669	6/1/2016	6/18/2016	10	0.018939	0.1654	0.0001	0.045	0.193333	39.6	1.327127	0.120472294
57_19	4.224736	5/8/2011	5/18/2011	1	0.018939	0.17275	0.0001	0.05	0.943333	23	0.508185	0.068874294
68_20	12.6	10/22/2017	11/2/2017	10	0.018939	0.17275	0.0001	0.05	0.313333	10.8	0.913952	0.160194356
66_19A	19.92715	9/11/2016	9/28/2016	1	0.018939	0.17275	0.0001	0.05	1.156667	84.6	1.443702	0.033581683

59_18	30.54795	5/9/2012	5/19/2012	10	0.018939	0.17275	0.0001	0.05	0.3	25.2	2.236891	0.216132229
52_3	31.68909	6/28/2007	7/8/2007	10	0.018939	0.17275	0.0001	0.05	0.493333	22.6	3.422498	0.111909461
51_11	22.25426	5/4/2007	5/24/2007	10	0.018939	0.17275	0.0001	0.05	0.283333	20.2	1.683927	0.164792527
52_7	21.97844	8/7/2007	8/17/2007	10	0.018939	0.17275	0.0001	0.05	0.326667	28.2	2.746962	0.190296205
52_6	28.96776	7/28/2007	8/7/2007	10	0.018939	0.17275	0.0001	0.05	0.286667	40	3.377731	0.396139684
52_8	25.18757	8/17/2007	8/27/2007	10	0.018939	0.17275	0.0001	0.05	0.233333	31.4	2.108646	0.117535481
52_4	22.69457	7/8/2007	7/18/2007	10	0.018939	0.17855	0.0001	0.045	0.44	28.8	3.730052	0.325680935
61_2	3.050586	11/28/2012	12/8/2012	1	0.018939	0.17855	0.0001	0.045	0.99	20.8	0.469358	0.18783165
68_17	28.1	9/19/2017	9/30/2017	10	0.018939	0.17855	0.0001	0.045	0.226667	44.6	2.538403	0.194248976
66_21A	32.91835	10/15/2016	11/1/2016	10	0.018939	0.17855	0.0001	0.045	0.23	135.6	5.077168	0.500344277
66_10A	33.54482	4/11/2016	4/28/2016	10	0.018939	0.17855	0.0001	0.045	0.39	84.6	5.664907	0.715252298
68_21	48.3	11/2/2017	11/13/2017	10	0.018939	0.17855	0.0001	0.045	0.37	20.8	2.033882	0.10272105
52_2	21.549	6/18/2007	6/28/2007	1	0.018939	0.17855	0.0001	0.045	0.146667	21.8	0	0
52_1	9.555278	6/8/2007	6/18/2007	1	0.018939	0.17855	0.0001	0.045	0.08	22.5	0	0
52_11	9.591366	9/16/2007	9/26/2007	1	0.018939	0.17855	0.0001	0.045	0.556667	23	0.458687	0.048973583
51_7	13.52312	4/4/2007	4/14/2007	10	0.018939	0.17855	0.0001	0.045	0.253333	27.4	1.944579	0.301799816
61_21	5.514221	6/6/2013	6/15/2013	2	0.018939	0.16665	0.0001	0.045	1.136667	28.6	2.022214	0.161768513
43_11	3.186901	6/7/2004	6/17/2004	1	0.018939	0.16665	0.0001	0.045	0.353333	23.4	0.079287	0.027614603
44_4	6.662726	9/1/2004	9/11/2004	1	0.018939	0.16665	0.0001	0.045	0.57	36.4	0.388354	0.117957502
68_19	30.8	10/11/2017	10/22/2017	10	0.018939	0.16665	0.0001	0.045	0.413333	15.6	1.849437	0.452937877
42_1	6.388895	10/14/2003	10/24/2003	1	0.018939	0.16665	0.0001	0.045	0.603333	38	0.447989	0.029489382
42_9	0.879266	1/2/2004	1/12/2004	1	0.018939	0.16665	0.0001	0.045	0.17	36	0	0
42_3	27.58248	11/3/2003	11/13/2003	10	0.018939	0.16665	0.0001	0.045	0.37	29.8	3.452258	0.173444128
44_1	22.42418	8/2/2004	8/12/2004	10	0.018939	0.16665	0.0001	0.045	0.183333	44.8	2.379835	0.347664292
59_21	2.591358	6/8/2012	6/12/2012	1	0.018939	0.1707	0.0001	0.02	0.826667	14.4	0.637695	0.073043656
42_4	23.45031	11/13/2003	11/23/2003	10	0.018939	0.1707	0.0001	0.02	0.31	16.4	1.52871	0.186375567
52_5	18.13986	7/18/2007	7/28/2007	10	0.018939	0.1707	0.0001	0.02	0.22	35.4	2.254575	0.348400703
60_2	0.92438	6/24/2012	7/4/2012	1	0.018939	0.1707	0.0001	0.02	0.183333	36.6	0.000546	0.000945308
68_18	21.8	9/30/2017	10/11/2017	10	0.018939	0.16665	0.0001	0.045	0.24	44.4	2.91277	0.575452189

Table 4: BSi data for the methods of determining the length of duration for dissolving BSi											
<u>Sample</u>	<u>dilution</u>	<u>filter blank</u>	<u>slope</u>	<u>sample filtered</u>	<u>blank</u>	<u>absorbance</u>	<u>sample volume</u>	<u>time</u>	<u>collection time</u>	<u>error</u>	<u>Silica flux [mg/m2/day]</u>
66_8	1	0.018939	0.17755	0.0001	0.005	0.45	92.3	0.5	17	0.01	0.017124588
66_8	1	0.018939	0.17755	0.0001	0.005	0.42	92.3	1	17	0.01	0.017124588
66_8	1	0.018939	0.17755	0.0001	0.005	0.46	92.3	2	17	0.01	0.017124588
66_8	1	0.018939	0.17755	0.0001	0.005	0.43	92.3	4	17	0.01	0.017124588
66_8	1	0.018939	0.17755	0.0001	0.005	0.51	92.3	6	17	0.01	0.017124588
58_5	10	0.018939	0.17755	0.0001	0.005	0.51	21.1	0.5	10	0.01	0.066550268
58_5	10	0.018939	0.17755	0.0001	0.005	0.51	21.1	1	10	0.01	0.066550268
58_5	10	0.018939	0.17755	0.0001	0.005	0.56	21.1	2	10	0.01	0.066550268
58_5	10	0.018939	0.17755	0.0001	0.005	0.49	21.1	4	10	0.01	0.066550268
58_5	10	0.018939	0.17755	0.0001	0.005	0.55	21.1	6	10	0.01	0.066550268